Recent developments in carbon nanomaterial sensors

Chem Soc Rev

Recent Developments in Carbon Nanomaterial Sensors

Journal:	*Chemical Society Reviews*
Manuscript ID:	CS-REV-11-2014-000379.R1
Article Type:	Review Article
Date Submitted by the Author:	24-Mar-2015
Complete List of Authors:	Baptista, Frederico; University College Dublin, School of Chemistry Belhout, Samir; University College Dublin, School of Chemistry Giordani, Silvia; Italian Institute of Technology, Quinn, Susan; University College Dublin, School of Chemistry

Journal Name

RSCPublishing

ARTICLE

Recent Developments in Carbon Nanomaterial Sensors

Cite this: DOI: 10.1039/x0xx00000x

F. Baptista[a], S. A. Belhout[a], S. Giordani[b] and S. J. Quinn[a]*

Received 00th January 2012,
Accepted 00th January 2012

DOI: 10.1039/x0xx00000x

www.rsc.org/

Carbon nanomaterials are among the most broadly discussed, researched and applied of synthetic nanomaterials. The structural diversity of these materials provides an array of unique electronic, magnetic and optical properties, which combined with their robust chemistry and ease of manipulation, makes them attractive candidates for sensor applications. Furthermore, the biocompatibility exhibited by many carbon nanomaterials has seen them used as *in vivo* biosensors. Carbon nanotubes, graphene and carbon dots have come under intense scrutiny, as either discrete molecular-like sensors, or as components which can be integrated into devices. In this review we consider recent developments in the use of carbon nanoparticles and nanostructures as sensors and consider how they can be used to detect a diverse range of analytes.

Introduction

In the past decade nanomaterials have begun to emerge as a viable alternative to molecular sensors and biosensors. This has been become possible by coupling their inherent properties [1,2,3] with our established knowledge of molecular and biomolecular recognition.[4] In particular, carbon nanomaterials (CNMs) are among the most broadly discussed, researched and applied synthetic nanomaterials.[5,6,7,8,9,10,11] This is due to their diverse intrinsic electronic, magnetic and optical properties, chemical versatility and ease of manipulation, biocompatibility as well as their performance as a chemically robust platform. This latter property sets them apart from many other nanomaterials whose stability can be compromised by factors including temperature, high ionic strength and solvent stability. Consequently, there has been a sustained interest in the use of CNMs for sensing applications.[12, 13, 14]

CNMs exhibit huge diversity in structure, existing in allotropic forms such as, diamond, graphene, amorphous carbon, C60 and single-walled carbon nanotubes (SWNTs). These materials can be conveniently separated according to the number of dimensions greater than 100 nm *i.e.* zero-dimensional (0-D) nanoparticles, one-dimensional (1-D) nanotubes and two-dimensional (2-D) layered materials. The discovery of C_{60} fullerene can be considered as the starting point of the CNM revolution.[6] In particular, the redox chemistry of fullerenes has been used to develop electrochemical sensors. Closely related to C_{60} are carbon nanoonions (CNOs), which typically consist of a fullerene unit surrounded by concentric layers of graphitic carbon.[15] Key properties of CNOs include low density, high surface-to-volume ratio and good solubility.[16,17] However, only a few reports have been described in literature for the use of CNOs as sensors.[18,19]

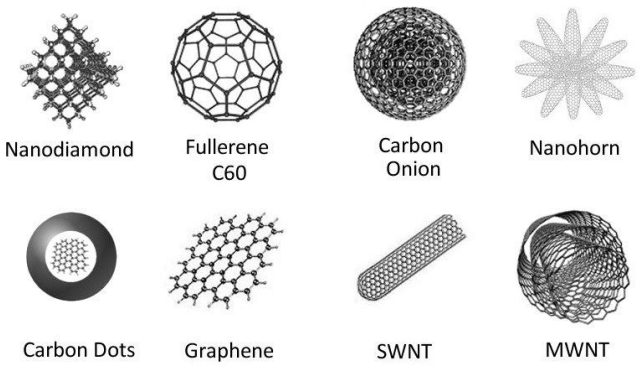

Fig. 1 Members of the carbon nanomaterial family.

Another type of CNM in this size regime are carbon nanodiamonds (CNDs), which combine the characteristics of diamond; optical transparency, chemical stability and biological compatibility, with the attractive nanomaterial properties of small size, large surface area and high adsorption capacity.[20, 21] One important additional feature of CNDs is their low toxicity.[22] CNDs are primarily made through the controlled detonation of explosives to yield core-shell particles with diameters of 4-5 nm.[23] The synthesis of fluorescent CNDs is also possible through the introduction of nitrogen vacancies (N-V centres), which are typically introduced by electron irradiation (2 MeV) of 100 nm CNDs followed by annealing (900°C) in vacuum.[23, 24] In addition, ultrasmall (1.6 nm) fluorescent NDs of roughly 400 carbon atoms and containing Si

vacancies have been also reported, which are also promising candidates for sensing. [25]

The most recent addition to the 0-D family of CNMs are carbon dots (Cdots), also referred to as graphene quantum dots (GQDs). The earliest reported syntheses of Cdots was by the laser ablation of a carbon target[26] and from candle soot.[27] Today Cdots can be prepared by pyrolysis[28], hydrothermal and[29] electrochemical treatments,[30] and microwave synthesis[31] of a wide variety of carbon sources such as foodstuffs, biomass and waste materials.[28–30,32–38] These methods provide access to Cdots whose luminescence spans the visible spectrum.[39,40] In particular, CNHs, CNDs and Cdots are attractive for in-vivo biosensing due to their biocompatibility.[12,24 41]

To date, the use of carbon nanotubes (CNTs) and graphene, and their related species, has received the greatest interest for sensing. Graphene comprises a single, layer of sp^2 carbon and as such can be considered the molecular parent of the sp^2 CNMs.[42] Graphene's ability to absorb light of all wavelengths coupled to its excellent electron transport properties has generated enormous interest.[43] Typically, graphene is prepared by mechanical and liquid phase the exfoliation of graphite;[44,45] recently large scale preparation of graphene using surfactants has been reported.[46] In addition to pristine graphene several surface treated forms such as photoluminescent graphene oxide (GO)[47] and reduced graphene oxide (RGO) have also been used for sensing applications.[48, 49]

Carbon nanotubes, are tubular structures of rolled-up sheets of graphene comprising single-wall (SWCNTs) and multi-wall (MWCNTs) species.[7] SWCNTs exhibit metallic, semi-metallic and semiconducting, properties which may be exploited for sensing applications.[12,14,50–53] These properties depend on the nature of the rolled graphene sheet, which dictates the chirality of the species. The general synthesis of CNTs employs chemical vapour deposition of carbon in the presence of a transition metal catalyst.[54] Closely related to SWCNTs are single-walled carbon nanohorns (CNHs).[10] These are conical structures with diameters of 2-5 nm and lengths of 40-50 nm which typically assemble into dahlia-flower like or bud-like aggregates with a diameter of about 100 nm. CNHs possess good porosity and high surface area which can be exploited for sensing applications.[10, 55] Importantly, CNHs can be produced in high yield in the absence of metal catalyst by either CO_2 laser ablation of pure graphite[10] or pulsed arc discharge of carbon rods.[56]

The purity of synthesised CNMs is an essential consideration for any possible sensing application. Two key considerations are the presence of (1) impurities which may interfere with the detection of analytes and (2) a polydisperse sample which influences both the optical properties and the ability to form ordered assemblies. Of the CNMs fullerene derivatives are the only members that can synthesised with precisely known composition. For example, CNTs must be rigorously purified to remove the transition metal catalyst species,[57,58, 59] Furthermore, in-vivo biosensing applications require the removal of carbonaceous fragments, which can act as reactive oxygen species.[60, 61, 62] The size dependent optical properties CNMs also necessitate the use of separation procedures to obtain monodisperse samples.[63] Techniques for the separation of chiral CNTs include ultracentrifugation[64] and gel permeation chromatography.[65] Centrifugation techniques have also been used for the length separation of CNTs[66] and the size-selective purification of dispersed graphene flakes.[67] In addition, Cdots have been separated from non-luminescent materials using C-18 HPLC.

In general, CNMs display poor solubility in aqueous solvents where they are prone to aggregation due to hydrophobic interactions. However, this can be addressed through surface functionalisation by covalent[68, 69] or non-covalent methods.[70–72] Surface modification is also used introduce receptor sites for sensing. A very useful summary of CNTs surface reactions for sensing applications was recently provided in a review article by V. Biju.[73] In the case of sp^2 carbon species covalent functionalisation results in the permanent disruption of the π-electronic network which can influence the optical properties of the material. This can be avoided through the use of non-covalent methods which largely reply on π-π stacking interactions between the CNM surface and molecules such as pyrenes and porphyrins and can be used to modulate the CNM optical properties. Significant progress in this area has been achieved by the groups of Dai[74] and Stoddart.[75]

Chemical sensors possess a receptor which transforms physical, chemical or biochemical information into an energy form that can be measured. CNM based sensors may constitute either discrete particles (common for optical based sensors) or particles within a composite device or an array (common for electrochemical based sensors).[76] The diverse intrinsic properties of CNMs give rise to range of sensing mechanisms. The most common of which are, (1) electrical, where binding of the analyte changes the dielectric environment; (2) electrochemical, due to a redox process at the CNT surface and optical mechanism such as fluorescence quenching, where there is a loss of emission due to the interaction between the CNM and the analyte.

The sensing of small molecules including drugs, metal ions, gaseous analytes and biomolecules is vitally important to the areas of health, the environment, food and safety and beyond. The sensing of metal ions such as Fe^{2+}, Zn^{2+}, Ca^{2+}, Na^{+}, K^{+} and Mg^{2+}, is very important in the area of health. Other important analytes for health include glucose, neurotransmitters such as dopamine, gene sequences for disease diagnosis, and illegal drug molecules. Sensors are also required for environmental monitoring of metal ion pollutants and toxins where the detection of these pollutants at trace amounts, especially mercury, is critically important.[77,78] In this review, developments in the use of CNM based sensors for the detection of a range of analytes will be explored. A comprehensive review of all CNM sensors is beyond the scope of this review and accordingly, we have highlighted the key milestones and the current state of the art together with examples from the recent literature with particular emphasis placed on research activity in the last two years.

Fullerene Sensors

Functionalised fullerenes and modified electrodes containing fullerenes have been used to detect a wide range of molecules including fluoride ion,[79] glucose[80–82], hydrogen peroxide[83], and various organic vapours.[84,85] For a comprehensive treatment of the functionalisation of fullerene, and its potential biosensing applications, readers are directed to the review prepared by Afreen *et. al.*[86] One example of a fullerene-based optical sensor for the selective detection of F^- ions was recently reported by Xu *et. al.*[79] The sensor comprises an open-cage fullerene with an enamine moiety at the opening (**1**), see Figure 2. The presence of F^- ion results in a redshift of the fullerene absorption peak from 717 nm to 823 nm. The quantification of fluoride ions in solution can be determined by measuring the ratio of $A_{823\ nm}/A_{717\ nm}$. Using a 10^{-5} M solution of (**1**) the F^- a detection limit of was found to be at the micromolar level.

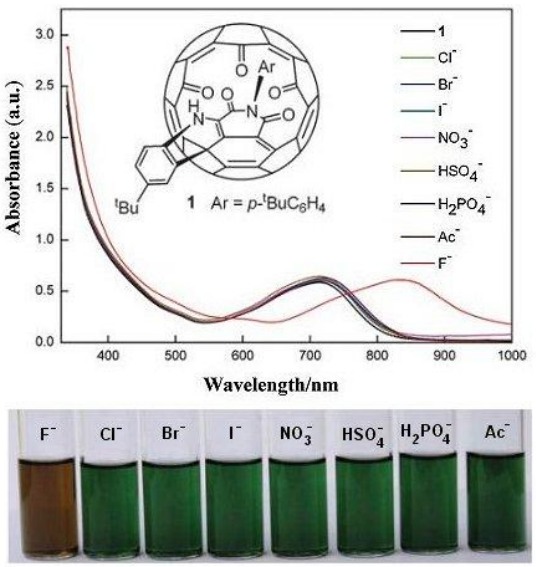

Fig. 2 Absorption spectra of **1** (10 μM) in the presence of excess anions (as their TBA salts) in $CHCl_3$. The corresponding colour changes are shown below. Reprinted with permission from Ref.[79] Copyright (2014) The Royal Society of Chemistry.

Carbon Nanodiamond Sensors

In common with other CNMs, CNDs require surface functionalisation in order to increase solubility and promote selective binding to the target analytes.[87] A unique property of CNDs is the ability to form emissive nitrogen-vacancy (N-V) defects where the fluorescence depends on the electronic spin state of the N-V centre.[88] The temperature sensitivity of these N-V centre spin states was recently exploited by Neumann *et al.* to prepare a fluorescent temperature probe.[89] N-V containing CNDs dispersed in polyvinyl alcohol were spin-coated onto a glass cover modified with a radio frequency controlled resonator. Fluorescent confocal microscopy was then used to measure temperature response of individual N-V centres. This CND-based sensor exhibited accuracy down to 1 mK. Interestingly, the combination of precision, resolution and photostability can also be applied to the measurement of the heat produced by chemical interactions.

CND temperature probes for use in living cells have been reported by Lukin and co-workers.[90] To demonstrate that this technique is compatible with living cells, a mixture of CNDs and gold nanoparticles (AuNPs) were introduced into the cells. The uptake of gold nanoparticles provided a local heat source in human embryonic fibroblast cells, which was controlled by laser irradiation. This probe was capable of detecting temperature variations of 1.8 mK, see Figure 3a-b. This study demonstrated the potential use of biocompatible CNDs as robust temperature sensors that combine sub-micrometre spatial resolution and sub-degree thermal sensitivity.

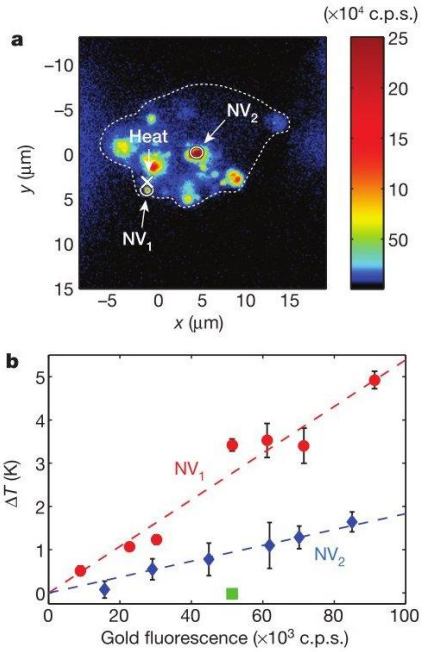

Fig. 3 NDs for thermal sensing. (a) Confocal scan of a single cell under laser excitation at 532nm, with collection at wavelengths greater than 638nm. The crossmarks give the position of the AuNPs used for heating, and circles represent the location of the ND (N-V1 and N-V2) used for thermometry.[90] (b) Monitored temperature dependent fluorescence. (a-b) Reprinted with permission from Ref. [90] Copyright (2013) Macmillan Publishers Limited.

In addition to the emissive properties of CNDs N-V centres, their spin relaxation properties offer a unique sensing capacity compared to other CNMs. An elegant example of this mode of sensing was described in 2013 by Ermakova *et al.* when they reported a magnetic field sensor for ferritin.[91] Non-covalent binding of the ferritin (5 nm) to 20 nm CNDs was achieved through electrostatic interaction between the CNDs surface COO^- groups and the amino groups on the protein. The spin states of single N-V centres are sensitive to the presence of the Fe^{3+} atom in the ferritin core (S = 5/2) whose presence leads to a shortening of spin coherence time, T_2, and relaxation time, T_1, by an order of magnitude compared to nonfunctionalised CNDs, see Figure 4. In addition, the modulation of N-V centre emission (630-750 nm) has been used for the detection of weak magnetic field by Maze *et al.*.[92]

In a related study the presence of gadolinium spin labelled lipids could be detected in an artificial cell membrane by monitoring the spin relaxation of individual CNDs.[93] In this approach, the magnetic detection of gadolinium spin labels is possible due to the change in the relaxation time T_1 of the CND N-V centres, see Figure 5. These results demonstrate that even a few molecules have a strong and quantifiable impact on the spin properties of a single N-V centre and demonstrate the

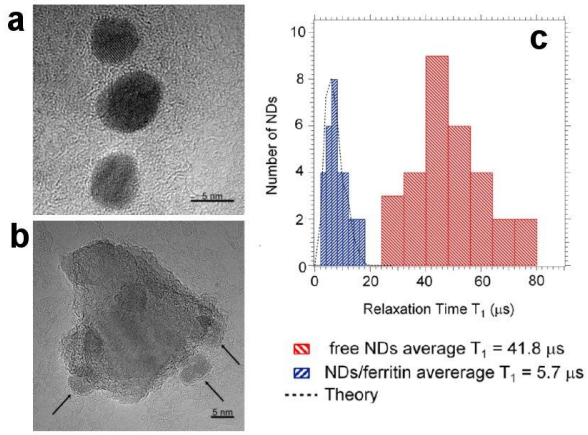

Fig. 4 HRTEM images of (a) ferritin molecules with an iron core. (b) ND bound ferritin. (c) Electron spin–lattice relaxation time T_1 of N-V in NDs as received (left) and in ferritin coated NDs (left, inset). Statistical distribution of the T_1 for free nanodiamonds (blue bars) and for ferritin coated nanodiamonds (red bars). Reprinted with permission from Ref.[91] Copyright (2013) American Chemical Society.

feasibility of CNDs to act as nanoscale sensors capable of reporting on nanovolume spins in solution including cell compartments.

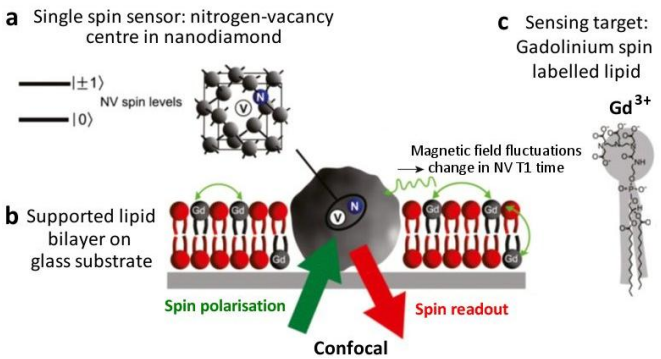

Fig. 5 (a) (Single N-V optical centre within the ND. (b) Supported lipid bilayer (SLB) formed around a ND immobilized on a glass substrate. (c) SLB Gd spin-labelled lipids are introduced into the SLB and magnetic field fluctuations arising from Gd spin labels affect the quantum state of the NV spin, measured through the N-V relaxation time, T_1. Reprinted with permission from Ref.[93] Copyright (2013) National Academy of Sciences.

Due to their hardness and transparency CNDs are commonly used in films and coatings. In 2010 Ahmad *et al.* reported a microelectromechanical chemical sensor for 2,4-dinitrotoluene (DNT).[94] The CNDs based sensor was prepared by coating a silicon cantilever with partially carboxylated and hydroxylated detonation CNDs. The CND surface COOH groups bind to the electron deficient oxygen atoms of the DNT nitro group. The analyte chemisorption was monitored by changes in the cantilever's resonance frequency, which exhibited a sensitivity of 0.77 pbb/Hz.

Carbon Dots Sensors

Fluorescent Cdots have emerged as highly promising sensor materials and a number of reviews have been written describing the sensing applications. In light of this the next section focuses on more recent developments.[39,40,95,96]

Carbon dots for cation and anion sensing

Fluorescent Cdots have come to the fore in recent years as fluorescent probes for the detection of many cations, including Hg^{2+},[29,33,97–100] Fe^{3+},[28,31,34,101–103,104] Cu^{2+},[35,36,103] Zn^{2+},[105] Al^{3+},[106] Ag^{+},[107,108] K^{+},[37] Be^{2+} [109] as well as number of anions, including oxalate,[110] iodide,[111] hypochlorous acid (HClO),[112] nitrite[38] and superoxide.[30] The sensing of Fe^{3+}, Cu^{2+} Be^{2+}, Hg^{2+} and HClO has been achieved using as synthesised carbon dots possessing oxidised surface groups. In the case of Fe^{3+}, it has been postulated that Fe^{3+} coordination to the Cdot surface phenolic hydroxyl groups results in fluorescence quenching due to the nonradiative electron-transfer of an excited-state electron from the Cdot to the d orbital of the Fe^{3+} ion.[101] Electron transfer facilitated Cdot quenching has also been used to detect Hg^{2+} ions, by Zhou *et al.*[113] and subsequently by Liu *et al.*[98] This method of detection has led to very selective and sensitive sensors for Be^{2+}, Cu^{2+}, Fe^{3+} and Hg^{2+} ions with detection limits of 23 μM,[109] 5 nM,[103] 1.7 nM [34] and 1 fM[98] reported respectively.

The quenched or "turned-off" fluorescence observed in the presence of one analyte can be restored in the presence of species with a higher affinity for the Cdot surface groups. This method has been used to for the selective detection of iodide ions in solution which were found to displace the surface the Hg^{2+} ions.[111] Here the re-growth in the fluorescence of the carbon dots was used to monitor the presence of iodide. A very attractive feature of Cdots is their biocompatibility which can be exploited to develop of in-vivo biosensors. The cell presents a particularly competitive environment in which to sense biologically important ions. Therefore, the Cdot surface must be modified with suitable receptor molecules. An elegant example of this was reported by Zhang *et al.* who prepared a nanosensor comprising Cdots functionalised with a zinc responsive quinoline derivative, see Figure 6a.[105]

The binding of Zn^{2+} ions by the nanosensor results in a shift in the fluorescence from weak blue (450 nm) to a strong green colour (510 nm), which is observable by the naked eye. Importantly, the limit of detection of 6.4 nM for the nanosensor was found to be significantly lower than the detection limit of 270 nM reported for the free quinoline molecule. This improvement was attributed to the large amount of recognition units around each carbon dot. Selectivity was tested against a wide range of both metal ions and amino acids, with little to no interference. In addition, the presence of the amine-rich capping ligand at the Cdot surface was found to convey high cell membrane permeability which allowed in-vivo imaging of Zn^{2+} in HeLa cells, see Figure 6b.

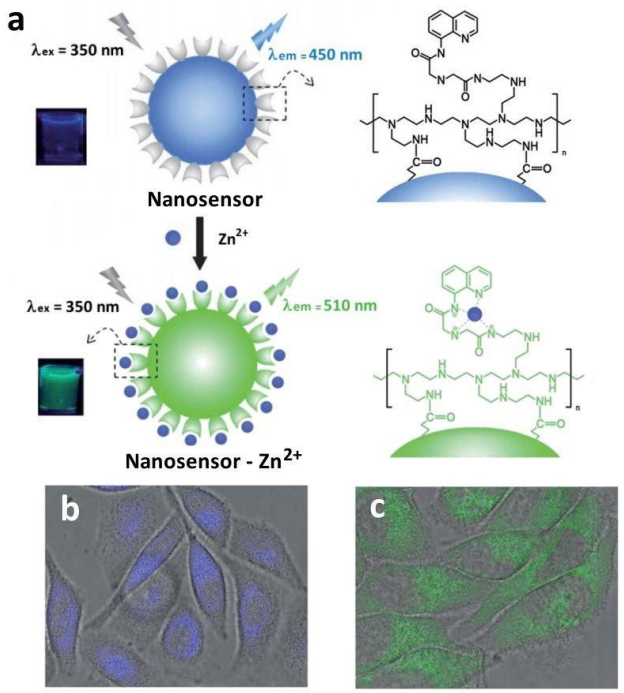

Fig. 6 (a) Schematic showing the coupling of the quinoline modified Cdot sensor for detection of Zn^{2+} ions. Overlay of bright-field and fluorescence images images of HeLa cells incubated with 250 mg mL^{-1} of the nanosensor before (b) and after (c) the exogenous Zn source treatment (addition of 50 mM $ZnCl_2$). Reprinted with permission from Ref[105] Copyright (2014) The Royal Society of Chemistry.

In a further development of Cdot sensors, Wei *et al.* recently used Cdot fluorescence to report on the selective detection of K^+ ions by graphene modified with an 18-crown-6-ether.[37] Cdots modified with an alkyl ammonium molecule were found to bind to the crown ether through known cation–ligand interactions. These interactions bring the Cdots in close proximity with the graphene surface where the Cdot emission is quenched by a fluorescence resonance energy transfer (FRET) process. Introduction of potassium ions causes the Cdot to be displaced from the crown ether-modified receptor and results in the detection of Cdot fluorescence, see Figure 7.[37] This process was shown to be selective towards K^+, with the ratio of K^+ to Na^+ on the surface being nearly 35-fold. It was also shown that the K^+ ion had no affinity to the bare graphene. This method has been used to detect potassium ions in concentrations as low as 10 μM.

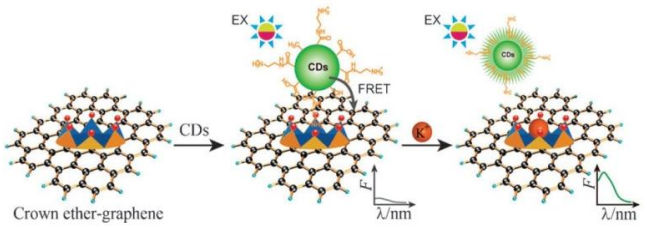

Fig. 7 Schematic illustration of the FRET model based on Cdots-graphene and the mechanism of K+ determination. Reprinted with permission from Ref.[37] Copyright (2012) The Royal Society of Chemistry.

One very important ion implicated in cellular function is the superoxide anion $O_2^{\bullet-}$. Superoxide is the primary reactive oxygen species (ROS) and its presence $O_2^{\bullet-}$ is implicated in a number of diseases such as cancer and diabetes. and recently a Cdot based ratiometric sensor for $O_2^{\bullet-}$ was reported.[30] In this system the Cdot fluorescence at 525 nm remains unchanged in the presence of $O_2^{\bullet-}$ and is used as the reference signal. However, the reaction of the surface immobilised hydroethidine group with $O_2^{\bullet-}$ results in emission at 610 nm, which increases with increasing superoxide, see Figure 8. The specificity of the reaction allows selective sensing of $O_2^{\bullet-}$ in preference to other reactive oxygen species such as including $^{\bullet}OH$, H_2O_2, $^1O_2$, $ONOO^-$ as well as metal ions. Furthermore, the system demonstrated long-term stability against pH changes and continuous light illumination. The dual emission behaviour was also detected by particles uptaken by HeLa cells for which good cell-permeability and low cytotoxicity were observed. The in-vivo monitoring of $O_2^{\bullet-}$ was confirmed by initiating superoxide formation in cells that pre-treated with an $O_2^{\bullet-}$ scavenger.

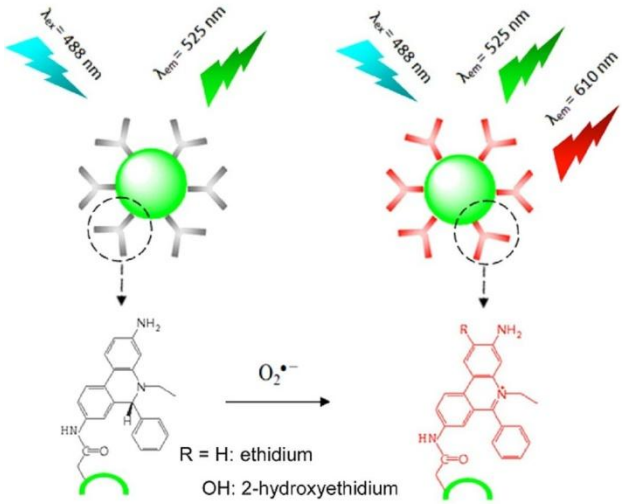

Fig. 8 Schematic representation of the working principle of a ratiometric fluorescent CD-HE biosensor for $O_2^{\bullet-}$ (Reprinted with permission from Ref.[30] Copyright (2014) The Royal Society of Chemistry.

In addition to Cdot fluorescence-based metal ion sensors, it is also possible to exploit the catalytic and redox properties of Cdots for the detection of metal ions. Shen *et al.* describe a process in which silver nanoparticles of ~ 3.1 ± 1.5 nm are formed by the reduction of Ag^+ ions by phenol hydroxyl groups at the Cdot surface, see Figure 9.[108] The nanoparticles result in

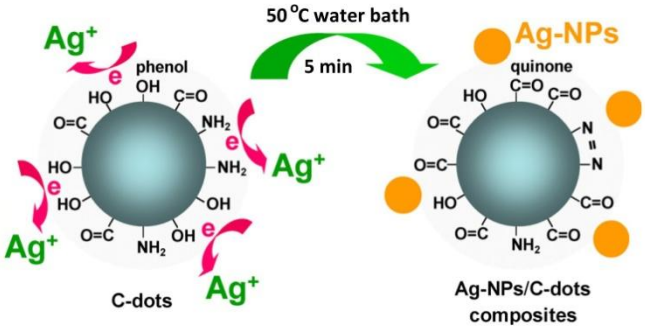

Fig. 9 Scheme showing the formation of AgNPs using carbon dots as the reducing agent. Reprinted with permission from Ref.[108] Copyright (2013) American Chemical Society.

Table 1: Table summarising the detection of cations by CD systems. (LR= linear range, LOD = limit of detection)

Carbon Dot Sensor Type	Detection Type	Target Cation	LR	LOD	Ref.
Cdots (refluxing poly(ethylene glycol))	Fluorescence Quenching	Hg^{2+}	1×10^{-6}-10 nM	1 fM	98
Cdots (hydrothermal treatment of honey)	Fluorescence Quenching	Fe^{3+}	0.005- 100 μM	1.7 nM	34
Cdots (microwave treatment of ionic liquids)	Fluorescence Quenching	Cu^{2+}	n.a.	5 nM	103
Cdots (hydrothermal treatment of uric acid and citric acid)	Fluorescence Quenching	Be^{2+}	23.3 – 100 μM	23.3 μM	109
Cdots (hydrothermal treatment of chitosan)	Resonance Light Scattering	Ag^{+}	0.5 – 6 μM	0.13 μM	108
Crown ether-modified graphene/Cdots prepared from candle soot	Fluorescence	K^{+}	0.05 – 10 mM	10 μM	37
Quinoline derivative functionalised Cots prepared by pyrolysis of citric acid and polyethyleneimine	Fluorescence Shift	Zn^{2+}	0.1 – 20 μM	6.4 nM	105
Quercetin modified Cdots by hydrothermal treatment of citric acid and diethylenetriamine	Fluorescence Shift	Al^{3+}	1- 60 μM	558 nM	106

resonant light scattering (RLS) at 340 nm. A linear relationship was found between the changes in the RLS and the Ag^{+} concentration, leading to a limit of detection of 0.13 μM for the Ag^{+}. A summary of Cdot cation sensors are given in Table 1.

Carbon dots for small molecule and drug sensing

Cdot systems have been used to detect a range of drugs and small molecules including: tetracyclines,[114] melamine,[115] hydrogen peroxide,[115,116] 2,4-dinitrophenol,[117,118] picric acid,[118] amoxicillin[119] and pentachlorophenol.[120] An elegant example of this was reported by Yang *et al.* who demonstrated the selective and sensitive detection of tetracyclines, which are a family of antibiotics.[114] The carbon dots formed in this detection system come from a one-pot synthesis that utilizes an automatic reaction between L-cysteine, P_2O_5 and water to prepare cyan emitting Cdots. The limit of detection for the different tetracyclines varied from 4.2 – 7.5 nM, with the linear range typically going from 0.02 – 8 μM. The carbon dots also showed very good recovery % when te tracycline was both spiked in human urine (96 – 110%) and when it was used to quantitatively measure the amount of tetracycline in a pharmaceutically supplied tablet (98.8 – 102.4 %).

In a more sophisticated system Qian *et al.* described the use of Si-doped Cdots as multi-functional sensors for both H_2O_2 and melamine detection using a 'turn-off turn-on' mechanism.[115] The Si-doped Cdots, synthesised via a hydrothermal method using $SiCl_4$ as the Si-source and hydroquinone as the carbon source, are shown to be effectively quenched upon the addition of H_2O_2 the system. The quenching of the fluorescence is found to be linear with increased H_2O_2 (25 and 200 μM) with a detection limit of 2.1 μM. The subsequent addition of melamine results in a reaction with H_2O_2 and restores the fluorescence of the Si-doped carbon dots.

Carbon dots for biomolecule sensing

Integrated systems containing cdots have been used in recent times to detect a wide range of biomolecules, including; cholines,[121] gluthathione,[122] hydrogen sulfide,[123] L-cysteine,[124] ovalbumin,[125], DNA,[126,127] ascorbic acid,[128,129] cholesterol,[130] histone,[131] dopamine,[132] human carcinoembryonic antigen (CEA)[133] and glucose.[134,135] These have been detected a variety of ways, including fluorescence quenching,[121,134,135] fluorescence 'turn-off turn-on' methods,[122–125,127–129,131] modified electrodes[132,133] and target recognition.[126]

In particular, Shen and Xia presented a simple and effective system which utilizes boronic acid functionalised carbon dots for the detection of glucose in the blood. The boronic acid functionalised particles were synthesised in a one-step "synthesis-modification integration strategy" using a phenyl boronic acid molecule as the sole precursor.[134] Thus the nanoparticles prepared possess a high volume of boronic acid groups at the Cdot surface, which act as glucose receptor sites. In the presence of glucose cross-linking of carbon dots occurs due to binding to receptor sites on different particles, which causes quenching of the Cdot emission, see Figure 10. This method has proved to be very sensitive, with a limit of detection of 1.5 μM and selectivity against a range of interfering carbohydrates including sucrose, fructose, lactose, maltose and a range of amino acids and other biomolecules. However, as the linear range of the sensor (9 to 900 μM) is somewhat lower than *in-vivo* blood glucose levels, sample dilution is necessary for assaying to avoid any interference from the blood/serum matrix.

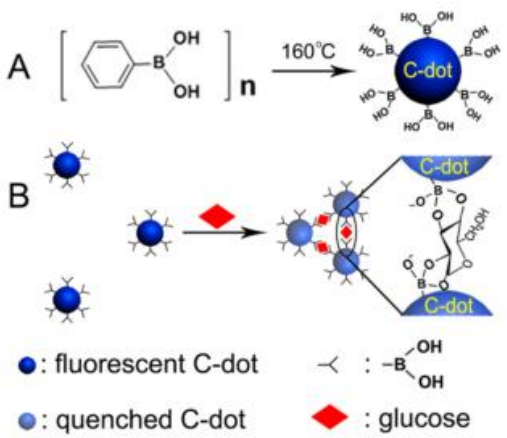

Fig. 10 Schematic showing the (A) formation of the boronic acid functionalised carbon dots and (B) working principle for the sensing of glucose. Reprinted with permission from Ref.[134] Copyright (2014) American Chemical Society.

One example of the use of an 'off-on' sensor was demonstrated by Tripathi *et al.*[130] who recycled soot, an environmental pollutant, from a diesel engine to form water soluble fluorescent Cdots possessing surface COOH groups. The Cdot surface was then modified with positively charged methylene blue (MB) molecules through electrostatic binding, which act to quench the Cdot emission. This emission was found to be restored in the presence of cholesterol molecules which bind to the MB molecules with a stronger affinity than the Cdots.

A further example of the application of Cdots for cellular sensing was reported by the Wu group who, building from the work of Chang, developed a FRET ratiometric sensor Cdot for H_2S detection in aqueous media and live cells. The sensor employed Cdots modified with a azo-naphthalimide probe that is reduced to an amino-naphthalimide in the presence of H_2S. In the absence of H_2S the blue emission of the Cdot is detected. However, the formation of the amino-naphthalimide generates a suitable energy acceptor of the Cdot emission, which yields green FRET emission at 526 nm see Figure 11. The biocompatibility and small particle size (5nm) of the Cdots facilitated cellular uptake with no observed toxicity. Significantly, the appearance of the green emission was used to image the presence of H_2S in HeLa (human cervical cancer) and L929 (murine aneuphloid fibrosarcoma) cells.[136]

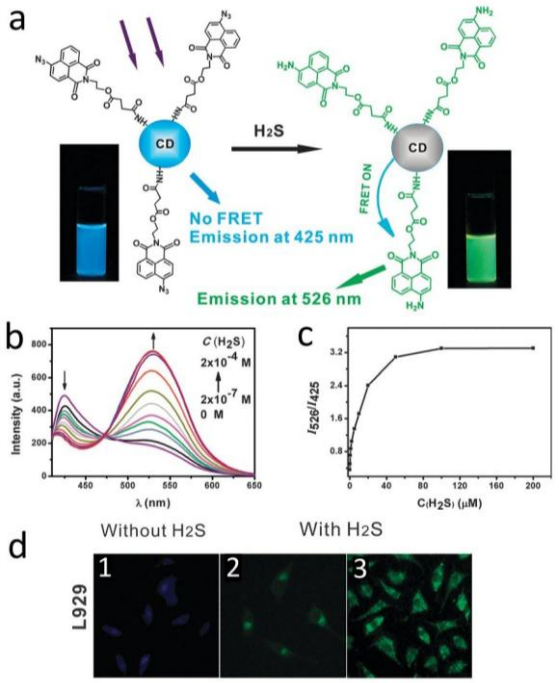

Fig. 11 (a) Schematic illustration for the structure of the carbon-dot-based sensor and its ratiometric detection of H_2S. (b) Fluorescence spectra of the CD-based sensor (concentration:0.45 mg mL^{-1}) in the presence of different amounts of H_2S; (c) fluorescence intensity ratio of the CD-based sensor as a function of H_2S concentration in HEPES buffered (pH 7.4) water–ethanol (3 : 1, v/v) (λexc = 340 nm). (d) Fluorescence imaging of HeLa and L929 cells incubated with the sensor before (1) and after (2, 30 mM; 3, 100 mM) treatment with H_2S. Reprinted with permission from Ref.[136] Copyright (2013) Royal Society of Chemistry.

Carbon Nanotube Sensors

Since their discovery CNTs have attracted tremendous interest from the scientific community due to their unique physical and chemical properties. The optical and electronic properties taken together with the structural properties make SWNTs and ideal material for generating nanostructures suitable for an array of sensing applications.[12,14,50–53] In this section we aim to highlight some of the key milestones to date and survey recent advances in the use of CNTs for sensing.

Carbon nanotube sensing of gaseous analytes

The detection of gaseous analytes, such as NH_3, NO_2, H_2, SO_2, CO and H_2S, by CNTs based sensors has been the subject of numerous studies which have been previously reviewed.[51] In particular, a number of these systems are based on electronic sensors, the development of which is described in the review by Jariwala *et al.*[14] One example of a powerful CNT sensing device is based on DNA-decorated CNTs, which allow detection of vapour analytes with similar chemical structure.[137] In this study, nanotube field effect transistors (FETs) were incubated with a 16 different DNA sequences. The resultant devices were screened against a family of structural isomers including enantiomers of limonene. The data from 600 devices revealed the ability of these sensors to discriminate molecules that differed in a single methyl group. In a subsequent study DNA-CNT sensors were reported to exhibit sequence specific binding affinity for analytes, including dimethylsulfone and isovaleric acid, at concentrations ranging from 48 to 360 ppb.[138] The sensitivity of the sensor was demonstrated in the ability of a particular sequence to discriminate between the three isomers of pinene, see Figure 12 (a-b). This discrimination coupled with response within seconds to ppb concentrations marked a significant development on previous sensors.

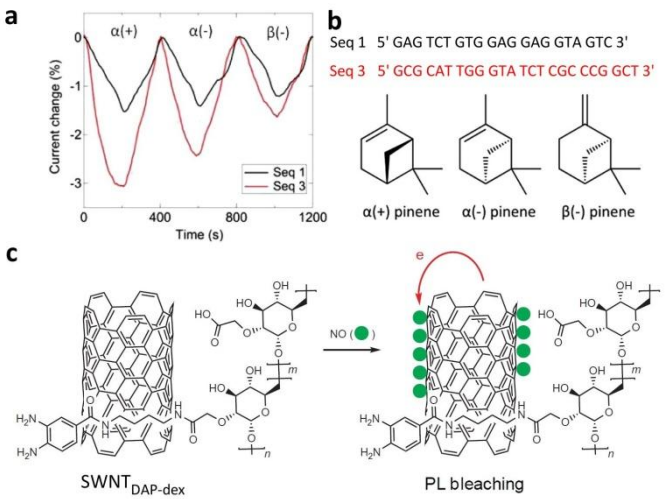

Fig. 12 NT detection of gaseous analytes. (a) Sequence dependent sensor responses to the introduction of pinene at 130 ppm concentration. (b) Sequences used in the study and the chemical structures of the pinene isomers. (c) Schematic illustration for NO detection using SWNT/polymer hybrid. (a-b) Reprinted with permission from Ref.[138] Copyright (2013) American Chemical Society. (c) Reprinted with permission from Ref.[139] Copyright (2009) Macmillan Publishers Limited.

In addition to electrochemical and electronic detection, optical sensors have also been developed for the detection of gaseous analytes. The optical detection of dissolved NO in solution by SWCNTs wrapped with 3,4-diaminophenyl-functionalised dextran was reported by the Strano group in 2009.[139] In this sensor the amino groups on the polymer coating act as a source of lone pair electrons which n-dope the semi-conducting SWNT. The resulting electron-rich nanotube is able to participate in direct charge transfer to NO, which results in NIR fluorescence quenching. This sensor was found to be selective for NO in the presence of other reactive nitrogen containing species, see Figure 12c.

In a related approach, the recognition properties of peptides have also exploited for the selective detection of analytes. In 2011 Heller *et al.* reported the use of a sensor comprising SWCNTs functionalised with peptides from the bombolitin family.[140] This chaperone sensor allowed the indirect detection of the analyte due to the near-infrared fluorescence quenching that arises due to changes in the polypeptide secondary structure upon binding. The peptides were found to be selective for a number of nitroaromatics including explosives.

Carbon nanotube sensing of biomolecules

The properties of CNTs have been exploited to develop a diverse range of biosensors. In these biosensors, CNTs can be modified with a biological sensing element, such as nucleic acids and peptides, and can also be modified with suitable groups capable of recognising biomolecules (*e.g.* proteins such as antibodies and enzymes), or monitoring bioprocesses. The biosensor design will also depend on whether the analysis is to be performed *in vivo* or *in vitro*. These factors have been explored in number of excellent reviews which have charted the progress of CNT biosensors.[141, 142, 142, 143]

An early example of a CNT-based electrochemical sensor for the detection of dopamine was reported by Britto and co-workers in 1996.[144] In this study the CNT electrode showed significant enhancement of detection over other carbon based electrodes. This was attributed to the increased surface area and the presence of pores due to the packing of the CNTs. Notably the authors also implicated the role of oxygen containing groups at the nanotube surface, which were formed during oxidation. Another significant development was the immobilization of glucose oxidase (GOx) onto the sidewalls of the SWCNTs for the detection of glucose, first reported by Besteman *et al.*.[145] The GOx-coated semiconducting SWNTs were found to act as reversible pH sensors and showed an increase in conductance upon adding glucose, suggesting the use as a sensor for enzymatic activity. Since then increasingly sophisticated electrochemical sensors have been reported. These sensors have been employed to detect toxins as well as drug molecules.

Toxic polyaromatic hydrocarbons (PAHs), which accumulate in the body, are an important class of analytes. Typically, the analysis of PAHs samples requires time-consuming, and expensive, pre-treatment. To overcome this, a CNT sensor based on the supramolecular recognition of 9-anthracenecarboxylic (9-ACA) was recently developed, see Figure 13. A β-cyclodextrin molecule was used as the recognition group, four of which were attached to 3,4,9,10-perylenetetracarboxylic acid. The perylene core allowed non-covalent assembly of the cyclodextrins at the SWNT surface through π-π interactions. Differential pulse voltammetry (DPV) measurements exhibited responses to 9-anthracenecarboxylic acid down to a detection limit of 0.65 nM.[146]

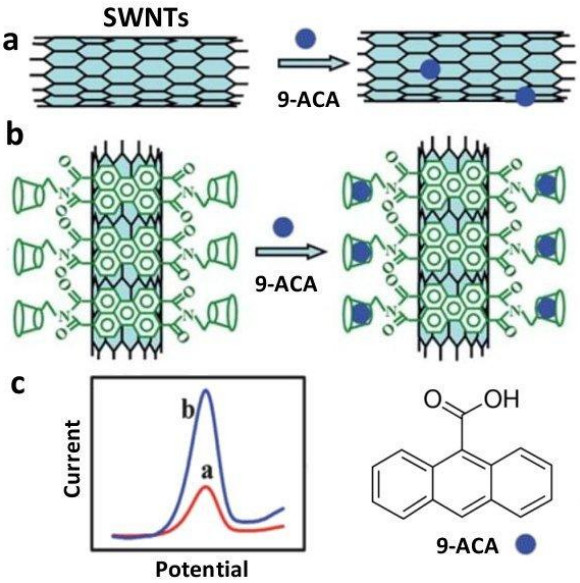

Fig. 13 SWNT-cyclodextrin based sensor for the detection of PAH toxins.[146] Schematic representation of the binding of 9-ACA to (a) bare and (b) modified SWNTs and (c) the improved electrochemical detection. (Copyright (2012) Royal Society of Chemistry.

An example of a CNT biosensor based on an electrochemical displacement assay was reported by Gu *et al.* for the detection of astralagoside IV, a component of the traditional Chinese herbal medicine Radix Astragali.[147] Here, MWCNTs were covalently decorated with boronic acid units capable of binding the astralagoside IV analyte and also the diol containing dye, Alizarin Red S (ARS), see Figure 14a.
The boronic acid groups are initially bound to the ARS dye molecule whose electroactivity results in a strong current compared with interferents present in Radix Astragali, such as glucose and sucrose. The change in the optical absorption of the ARS is used to report on the binding at the surface. However, in the presence of astralagoside the ARS dye is displaced, which results in a decrease in current.

SWCNT modified glassy electrodes were recently found to display high activity for the oxidation of Valacyclovir, which is the most common drug used for the treatment of the herpes zoster and cold sores.[148] In addition, the electroactivity of MWCNTs has also been exploited to prepare disposable sensors for the selective detection of cocaine in real life samples.[149] Linear regression treatments of readouts were used to resolve the overlapping oxidation peak for cocaine in the presence of codeine, paracetamol or caffeine. The detection of cotinine, a marker for exposure to tobacco, was also achieved through SWCNTs based sensor functionalised with a molecularly imprinted polymer (MIP).[150] CNTs were dispersed in a methanolic solution of PVP, poly-4-vinylphenol, and cotinine, which formed the MIP sheath. The template molecule

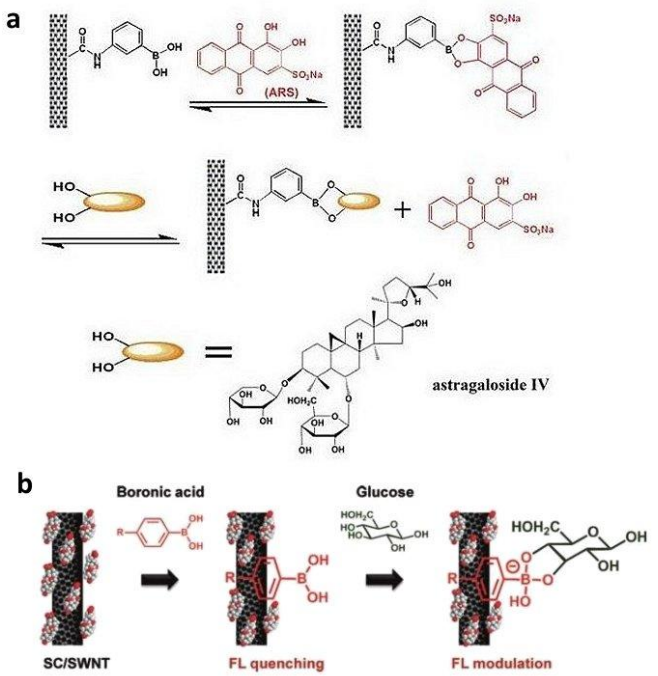

Fig. 14 Schematic representation of boronic acid modified CNT biosensors (a) CNT biosensor electrochemical displacement assay,[147] and (b) boronic acid modified SWCNTs for glucose detection by 'turn-on' fluorescence methods. (a) Reprinted with permission from Ref.[147] Copyright (2012) Royal Society of Chemistry. (b) Reprinted with permission from Ref.[152] Copyright (2012) American Chemical Society.

was subsequently removed and the sensor tested. Chromotographic analysis revealed the SWNT-MIP to have 200 % greater affinity for cotinine than the control SWNT-PVP sensor. The presence of cotinine generates a 900% increase in resistance compared to the non-imprinted electrode and was found to exhibit sensitivity down to 0.05 ppm.

CNT optical biosensors offer a powerful method of detection due to a number of factors. Chief amongst these is the tissue penetration afforded by the NIR window emission of semiconducting SWNTs (900-1300 nm). This is further advantaged by the fact that fluorescence measurements in this window are accompanied by less background autofluorescent signal in biological media and the fact that the separation of chiral nanotubes offers the potential to tune emission over a range of wavelengths. Furthermore, this emission is much more stable than quantum dots and dyes and is sensitive to changes in the local dielectric environment which can be used to report on molecular change.

Two examples of this approach have been used to develop a SWCNT-based glucose sensor. In an early example, a stable dispersion of (9,5) SWNTs bound to glucose oxidase was employed. In this system small molecules, such as $Fe(CN)_6^{3-}$, can permeate the surface coating and bind non-covalently to the surface. This binding results in emission quenching. However, the H_2O_2, generated from the reaction of glucose with the enzyme, partially reduces the surface bound $Fe(CN)_6^{3-}$ resulting in an increase in the emission.[151] This growth in emission then serves as a sensitive reporter of the H_2O_2 concentration. In a subsequent study, the Strano group employed sodium cholate stabilized (6,5) and (7,5) semiconductor SWCNTS modified with boronic acid derivatives, for glucose detection. Thirty different boronic acid species were anchored to the surface of SWCNTs through π-π interactions, which result in fluorescence quenching. Glucose binding to the boronic acid centre disrupts the π-π interactions and restores the emission, see Figure 14b.[152] Importantly, the boronic acid based sensors were found to display glucose detection in a physiologically important range of 5 to 30 mM.

The fluorescence response of DNA modified SWCNTs has also been used for simultaneous detection, *in vitro*, of four gentoxic analytes, including chemotherapeutic alkylating drugs, reactive oxygen species as well single molecule detection of H_2O_2.[153] The formation of a DNA coating at the surface results in strong SWNT luminescence which is diminished upon DNA damage. The modulation of nanotube emission could then be correlated to the concentration of the DNA damaging agent using principal component analysis.

Zhan *et al.* prepared a simple sensor using a fluorescently-label aptamer for the detection of cellular prion protein (PrP^C).[154] In this sensor the non-covalent modification of MWCNTs with the aptamer results in quenching of the fluorescence, which is then restored in the presence of PrP^C, see Figure 15. The sensor demonstrated good sensitivity capable of detection of at least 4.1 nM PrP^C. Furthermore, the sensor was found to exhibits excellent specificity for PrP^C in the presence of other proteins and amino acids.

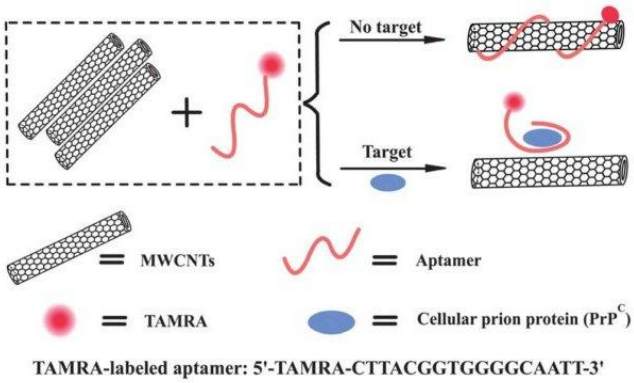

Fig. 15 Schematic demonstration of the mechanism of PrP^C detection based on the on–off noncovalent interaction of dye-labelled aptamers with MWCNTs. nIR fluorescence change from the SWNT occurs when the distance between the Ni 2þ quencher and SWNT is altered upon analyte protein binding. Reprinted with permission from Ref. [154] Copyright (2012) American Chemical Society.

Anh *et al.*, reported a label free approach capable of single protein-protein interaction detection using a SWCNT fluorescent sensor.[155] In this elegant approach, SWCNTs are embedded with a chitosan matrix bearing the chelator Nα,Nα-bis(carboxymethyl)-L-lysine, with this matrix SWCNTs can bind to hexahistidine-tagged capture proteins directly expressed by cell-free synthesis through Ni^{2+}. The intermolecular distance between Ni^{2+} ion and SWCNTs acts as a proximity quencher of the SWCNTs fluorescence upon docking of the analyte proteins. This label free based sensor exhibited a detection limit of 10 pM for an observation time of 600 s. A similar approach was followed for the detection of insulin by SWCNTs

functionalised with insulin-binding aptamer as molecular recognition element.[156]

A similar aptamer based approach has been reported by Wang *et al.* for the simultaneous, multicolour detection of Hg^+, Ag^+ and Pb^+ ions in solution.[157] Three different aptamers, capable of selective recognition of each ion, were labelled with fluorescein amidite, 6-carboxy-X-rhodamine and Cy5, for Hg^+, Ag^+ and Pb^+ respectively. The fluorescently labelled aptamers were then adsorbed at the surface of MWCNTs through π-π interactions, where their emission was quenched. The presence of the target cations was signalled by the appearance of restored dye fluorescence. This method exhibited a detection limit of 15 nM for Hg^+, 18 for nM Ag^+ and 20 nM for Pb^+. A similar detection limit for Hg^+ was achieved using a related system.[158] In addition, this method has been used for the detection of anions such as arsenite at the femtogram level in the lysosome of live cells.[159] A number of CNT biosensors for the detection of nucleic acids have also been reported. [160,161,162,163,164,165] These sensors have been typically based on changes in the system's luminescence due to conformational changes in the DNA structure or recognition of complementary sequences.

Carbon Nanohorns as Sensors

CNHs offer an attractive alternative to CNTs based sensors.[13] In particular the conical shape of carbon nanotubes confers different electronic properties to the material. Though CNHs are not inherently luminescent the presence of a large number of reactive sp^3 carbon edge sites allows labelling with various moieties. In addition, the opening of the cone-shaped tip provides further sites for covalent functionalisation.[166]

Carbon nanohorn electrochemical sensing

The metal free property of CNHs is a significant advantage over CNTs, for the preparation of electrochemical sensors where interference from residual metal impurities must be avoided. One of the earliest CNH sensors was an amperometric biosensor for glucose, reported by Liu *et al.* in 2008.[167] This sensor was constructed by immobilizing glucose oxidase into a Nafion-CNH composite film and using ferrocene monocarboxylic acid as a redox mediator. The glucose biosensor showed a linear response from 0 to 6.0 mM with a high sensitivity (1.06 μA/mM). It also exhibited good stability with constant readings obtained over a two week period.

Recently a bifunctional electrochemical CNH sensor capable of detecting hydrogen peroxide and hydrazine was also reported. This sensor employed CNHs non-covalently modified with a cobalt (II) schiff-base derived from salicylaldehyde (salen).[168] In this study the influence of the different sensor components were systematically analysed. Importantly, the presence of CNHs reduced the onset potential for oxidation of hydrazine by 200 mV compared to that for the standard glassy carbon electrode (GCE). This electroactivity was further enhanced by the presence of the Co(II) complex at the CNH surface (-400 mV). In addition, the electrocatalytic current was also found to increase and this was attributed to the complex acting as a good electron transfer mediator to shuttle electrons between the analytes and the electrode, see Figure 16. A good linear response in the range 1 to 96 μM was observed. The sensor exhibited a very fast response time (defined as 99% of the steady current) of within 5 s. This fast response was attributed to a combination of the ability of the hydrazine molecules to rapidly diffuse inside the SWNH pores and the excellent electrooxidation activity of the Co complex towards hydrazine. Additionally, the composite electrode exhibited electroactivity for hydrogen peroxide and resulted in a more positive reduction potential for with large enhanced peak current. Taken together these results demonstrate the versatility of CNH based electrochemical sensors.

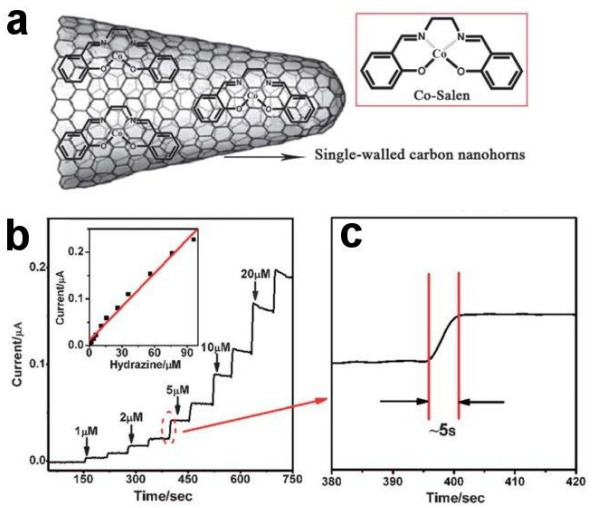

Fig. 16 (a) Schematic illustration of the structure of Co-salen/SWNHs nanosensor. (b) Amperometric responses of Co-salen/SWNHs/GCE with successive addition of hydrazine into PBS at +0.05 V, (inset the corresponding calibration plots) (c). Response time for detecting hydrazine. Reprinted with permission from Ref.[168] Copyright (2012) Royal Society of Chemistry.

Similarly, the electrocatalytic activity of CNHs towards the oxidation of dihydroxybenzenes has been used to detect food contaminants such as bisphenol A,[169,170] malachite green and triclosan.[170] CNH modified GCEs have also been used for the simultaneous detection of the dihydroxybenzene isomers, hydroquinone, catechol and resorcinol, with a detection limit of 0.1 μM, 0.2 μM and 0.5 μM respectively.[171] In a further development, Zhang *et al.* Recently reported the preparation of a biosensor based on xanthine oxidase immobilised on the surface of a CNH/gold nanoparticle (AuNP) hybrid, which was deposited on a platinum electrode.[172] This sensor exploited the high surface area of nanoporous structure of the CNHs with the electrocatalytic activity of gold nanoparticles. The CNH-AuNP sensor was found to exhibit good electrocatalytic activity for enzymatic products produced by oxidation reaction of xanthine and hipoxanthine with detection limits lower than 1 mM for xanhine and hipoxanthine.

The functionalisation of CNHs with receptor molecules offers the potential for increased selectivity of CNH electrochemical sensors. One example of this was reported by Dai *et al.* who used β-Cyclodextrin (β-CD) to prepare a CNH/β-CD electrochemiluminescent sensor for the detection of the

flavanone glycoside, naringin, see Figure 17.[173] CNH hybrids were assembled at the surface of a GCE where the luminal emission was found to increase two-fold at the GCE/CNHs surface compared to a bare GCE surface. The subsequent recognition of naringin by the immobilised β-CD resulted in a further increase in the electrochemiluminescence of luminal due to the presence of hydroxyl groups. The sensor allowed nanomolar detection of naringin with a detection limit of 0.8 nM.

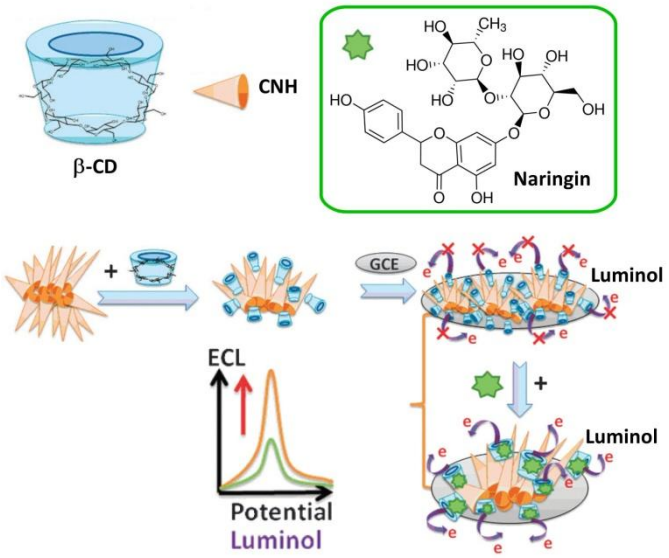

Fig. 17 Schematic representation of the fabrication and sensing principle of CNHs based ECL biosensor for naringin. Adapted with permission from Ref.[173] Copyright (2012) Royal Society of Chemistry.

A CNH electrochemical sensor employing a sandwich nanohybrid structure was reported by Tu *et al.* who modified an electrode surface with a CNHs-TiO_2-porphyrin nanohybrid. This low-cost amperometric sensor was applied to detect the presence of the antibiotic chloramphenicol (CAP).[174] The assembly of the hybrid was achieved through electrostatic binding of TiO_2 nanoparticles to COO^- groups, present on the porphyrin molecule and at the CNH surface. In this sensor the excellent electronic conductivity of the CNHs was exploited to enhance the transport of electrons produced by the porphyrin catalysed reduction of CAP. This transfer was further enhanced by the presence of bridging TiO_2 nanoparticles. The presence of CNHs was found to accelerate the electronic reduction of CAP over a wider concentration range then achieved by CNT based sensors.[175]

A number of CNH based immunosensors have also been developed. One of the earliest reported immunosensors was for the detection of microcystin-LR (MC-LR),[176] which is a highly toxic species released by cyanobacterial bloom. In common with many other CNH sensors the high surface area of CNHs was used to immobilise the recognition components. The immunosensor was prepared by depositing carboxylated CNHs at a GCE surface where they were subsequently bioconjugated to MC-LR. This electrode platform then participated in a competition with free MC-LR for binding to horseradish per-oxidase-labelled MC-LR antibody (HRP-labelled MC-LR), see Figure 18. The conditions of the competition assay were optimised to allow correlation of CNH/HRP-labelled MC-LR to the concentration of solution MC-LR. This concentration was correlated to the current detected from the enzymatic reaction of o-phenylenediamine in the presence of H_2O_2. Significantly, the current detected for the CNH based sensor was found to be twice as large as the CNT equivalent. The immunosensor displayed a wide linear response for MC-LR with a detection limit of 0.3 μg/L, which is less than the limit of 1 μg/L recommended by the World Health Organisation (WHO) for the level of MC-LR in drinking water. Furthermore, the sensor could be regenerated by washing and repeat incubation. This approach was also recently applied to determine the concentration of fibrinogen in human plasma and urine.[177]

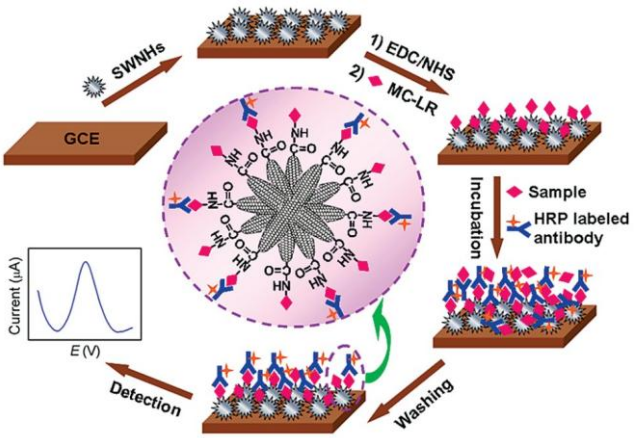

Fig. 18 Schematic representation of the fabrication and sensing principle of CNHs Reprinted with permission from Ref.[176] Copyright (2010) American Chemical Society.

In a further development, the electrocatalytic activity of CNHs was combined with an enzymatic biocatalylic precipitation (EBC) process to prepare a highly sensitive impedimetric immunosensor for α-fetoprotein (AFP).[178] This elaborate sensor was prepared from a number of components and the design was based on the use of two enzymes (bienzyme), namely horseradish per-oxidase (HRP) and glucose oxidase (GOx). The assembly of the sensor involved amide coupling of a secondary antibody to COOH groups at the surface of oxidized CNHs, see Figure 19. These CNHs were subsequently modified with the two enzymes. A primary antibody was also immobilized at the surface of a gold nanoparticle/graphene modified electrode. The recognition of the analyte results in the assembly of a sandwich configuration. The subsequent EBC oxidation of 4-chloro-1-naphtol (4-CN) by hydrogen peroxide in the presence of HRP results in the formation of an insoluble product on the electrode surface which results in an additional enhancement of the signal. This selective sensor exhibited a detection limit of 0.33 pg/mL for AFP.

A similar methodology was used for the construction of a multiplexed sensor incorporating AuNPs, streptadivin and CNHs for the detection of AFP and carcinoembryonic antigen.[179] The strategy followed here was based on the in situ growth of AuNPs on the carboxylated CNHs, followed by functionalisation with streptavidin, which allows the disposable

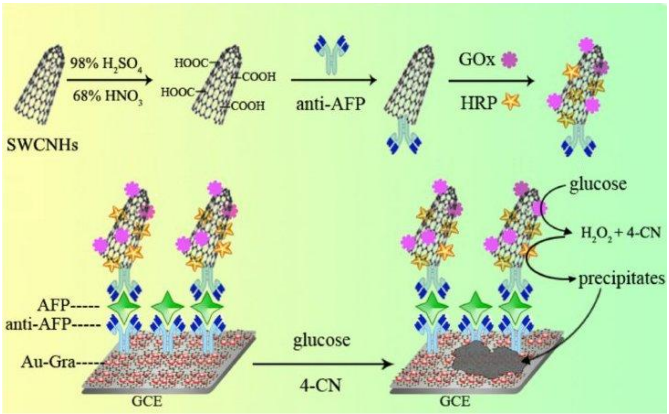

Fig. 19 Schematic diagrams for the preparation of CNHs–bienzyme–Ab2 bioconjugates Reprinted with permission from Ref.[178] Copyright (2014) Elsevier.

sandwich-type immunosensor to recognise biotinylated antibodies, this sensor presented a detection limit of 0.024 pg/mL and 0.032 pg/mL for AFP and carcinoembryonic antigen respectively.

Photoelectrochemical (PEC) sensing is a new analytical technique which uses light to induce electron transfer among the photoelectrochemical species and the electrode. Recently Dai *et al.*, reported a TiO_2-CNH hybrid sensor. In this device anatase TiO_2 mesocrystals (QOAMs) were used as the sensitising component. These ordered TiO_2 superstructures exhibit superior photocatalytic activity and possess quasi-octahedral shape, high porosity and large specific surface area. CNHs were employed to compete with the back electron processes in the anatase and thus improve the transport of photo-generated electrons to the electrode surface. The sensor was assembled by binding of the TiO_2 mesocrystals to a thiol group from CNHs functionalised with L-cysteine.[180] This arrangement was found to yield excellent transport of the anatase excited electron to the electrode resulting in a detectable photocurrent. However, this process is interrupted in the presence of an electron scavenger such as 4-methylimidozal; a food borne contaminant. This phenomena resulted in sensing the analyte to a detection limit of 30 pM.

Carbon nanohorn optical sensing

In the absence of intrinsic fluorescence, CNH optical based sensors generally rely on the ability of the CNHs to quench the fluorescence of an analyte.[181] An example of the use of this approach was used for the detection of DNA by Zhu *et al.*. Here a mix-and-detect strategy was demonstrated for fluorescent detection of a oligonucleotide sequence related to human immunodeficiency virus (HIV).[182] The detection mechanism of the sensor was based on the different binding affinity of CNHs for ss-DNA and ds-DNA. The dye-labelled probe sequence P_{HIV} has a high affinity for the CNH surface where it binds through π-π interactions, resulting in fluorescence quenching. However, this affinity is removed as the duplex is formed in the presence of the target sequence, T_1 (Figure 20). This sensing platform was found to selectively detect to single-base mismatches.

This same approach has also been applied to detect thrombin.[183] In this sesnor CNHs were non-covalently functionalised with a fluorescein labelled peptide whose fluorescence is quenched by the CNHs. In the presence of the thrombin protease the dye-labelled peptide is cleaved. The weaker interactions of the shortened fluorescein labelled peptide result in the release of the peptide and the recovery of the fluorescence. This sensor for thrombin exhibited a detection limit of 100 pM, which is the same detection limit exhibited by the sensor for thrombin using a fluorescein labelled aptamer.[181]

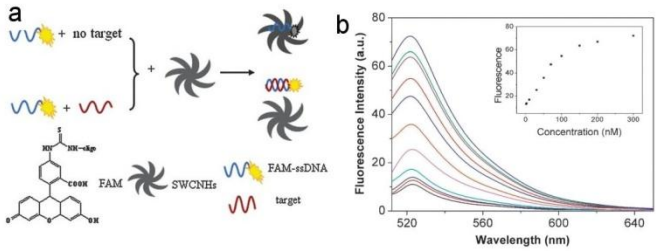

Fig. 20 (a) A schematic (not to scale) illustrating the CNHs-based fluorescent nucleic acid detection. (b) Representative fluorescence spectra for 50 nM PHIV in the presence of various concentrations of T_1 (from bottom to top): 0, 1, 2, 10, 30, 50, 70, 100, 150, 200, 300 nM. Inset: calibration curve for the fluorescence intensity of P_{HIV} versus T_1 concentration. Reprinted with permission from Ref.[182] Copyright (2012) Royal Society of Chemistry.

Graphene Based Sensors

Graphene has come to the attention of the sensing community in recent years due to its unique properties and a number of reviews have been published detailing graphene and its sensing applications.[184, 185, 186, 187] In particular, the properties of the 2-D material have been employed in electrochemical based sensors as they show promise for the preparation of cheap and easy-to-use sensors.

Graphene anion and cation sensing

Graphene has been utilized for the detection of several ions, including Ca^{2+}, [188,189] K^+, [189,190] Cu^{2+}, [191] Hg^{2+}, [192] F^-, [193] and nitrate.[194] The detection of these ions has largely relied on fluorescence and electrochemical methods. An aptamer approach similar to that employed by CNT ion sensors was developed by Xing *et al.* for the detection of K^+. This system comprised a dye labelled guanine rich DNA aptamer immobilised on a graphene oxide sheet, which is an excellent quencher of emission. In the absence of the target the DNA fluorescence is quenched. However, the presence of potassium ions results in a conformational switch in the guanine-rich DNA from random coil to G-quadruplex. In the quadruplex form the dye is located away from the graphene surface and emission is restored.[190] The fluorescence signal was further amplified in the presence of cationic conjugated fluorenylene phenylene polymer, PFP (poly [(9,9-bis(6'-N,N,N-trimethylammonium)hexyl)-fluorenylene phenyl dibromide]) which acted in two ways; firstly, in the absence of analyte it aids the immobilisation of the aptamer at the graphene surface and secondly, when the analyte is bound it participates in a

FRET process that results in a shift and strong increase in emission, see Figure 21. The use of the conjugated polymer in this way resulted in very low background fluorescence. The sensor demonstrated a limit of detection of 3.03 μM for K^+ with a linear range from 10 to 100 μM, with a high selectivity towards K^+.

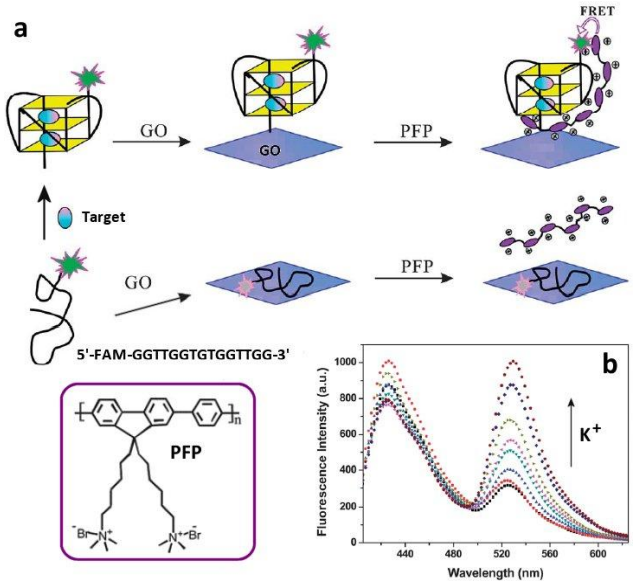

Fig. 21 (a) Schematic representation of a GO-based low background signal platform for the detection of K^+. (b) Fluorescence emission spectra of the assay system in the presence of different concentrations of K^+. Reprinted with permission from Ref.[182] Copyright (2012) Royal Society of Chemistry.

Electrochemical detection of ions by graphene has also been described, with two main families of graphene containing sensors being developed. These involve either modification of graphene with a ligand to increase the ion specificity or incorporation of the electrode with an ion-specific membrane (ISM).[194] An example of an electronic sensor for detection of heavy metal ions was recently reported. The sensing device monitors the current flowing in a layer of electrochemically reduced graphene oxide (ERGO) placed between two gold electrodes. In this study a glucose receptor molecule was linked (C_7 alkyl chain) to a pyrene group via imine binds. The pyrene molecule anchors the receptor to the ERGO surface via π-π interactions and the glucose hydroxyl groups as well as the imine groups can bind to Hg^{2+}. The presence of the mercury ions disrupts the ERGO charge carriers and causes a decrease in current. The addition of deionised water results in an increase in current and taking the ratio of these currents reveals a detection limit of 0.1 nM, which is significantly lower than previously reported detection limits and far below the maximum concentrations of Hg^{2+} allowed in drinking water by the WHO (30 nM).

Graphene sensing of drug molecules

A wide range of graphene sensors for drug detection have been reported, including sensors for pesticides,[195] cocaine,[196, 197] analgesics,[198,199] dopamine receptor agonists,[200,201] anti-migraine drugs[202,203] amongst others.[204–209] Two recently developed optical sensors for cocaine were based on aptamer-based fluorescence turn-on and turn-off mechanisms. Qiu *et al.* developed sophisticated sensor that uses a turn-on mechanism in tandem with an isothermal circular strand-displacement amplification (ICSDA) method.[196] The sensor uses a DNA hairpin sequence comprising two specific regions; the cocaine aptamer region and a region specifically designed to hybridize with a seven base DNA primer. The fluorescence in this system originates from SYBR Green 1 (SG) dye that binds to double-stranded regions of the DNA. In the absence of the analyte the hairpin sequence binds to the graphene oxide (GO) sheet resulting in fluorescence quenching, see Figure 22. However, in the presence of cocaine the aptamer undergoes a conformational which causes the hairpin to open and bind to the DNA primer. The addition of polymerase to this configuration releases the cocaine molecule and elongates the primer sequence, which generates a longer double-stranded DNA region that (1) has a low affinity for the graphene surface and (2) possesses a greater number of sites to bind the fluorescent dye and so amplifies the signal.

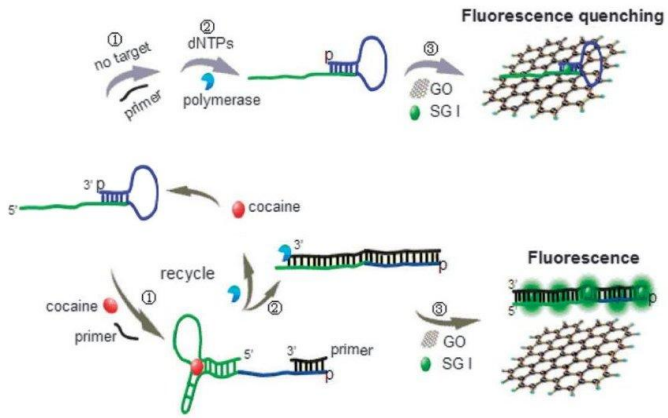

Fig. 22 Schematic representation of the label-free fluorescent aptamer-based sensor method for cocaine detection based on GO and hairpin elongation. Reprinted with permission from Ref.[196] Copyright (2013) Royal Society of Chemistry.

In a related study, Shi *et al.* took advantage of the inherent fluorescence of graphene oxide to prepare a fluorescence-off sensor.[197] Here, negatively charged graphene oxide (GO) was immobilized on a positively charged glass slide to which an amine modified cocaine aptamer is attached. A second cocaine aptamer functionalised with gold nanoparticles (AuNPs) is then introduced. In the presence of cocaine, a three way junction is formed which locates the AuNPs close to the GO surface, quenching the graphene fluorescence through electron transfer. The results for the two methods of cocaine detection are comparable. While the turn-off method has the slightly better limit of detection, 100 nM versus 190 nM for turn-on, the turn-on method benefits from the ability to monitor the appearance of fluorescence, rather than to determine the percentage that is quenched.

Electrochemical detection of drug molecules by graphene based sensors is most commonly achieved using the conventional three electrode system to exploit the charge carrier dynamics of graphene. The method of using graphene modified

GCE has been employed to detect a range of drugs including pramipexole,[201] cabergoline,[200] valganciclovir,[209] L-Dopa[207] and caffeine.[208] These systems show good sensitivity with the limits of detection ranging from the lowest of 3.1 nM for valganciclover to 91 nM for caffeine. Jain and Seetharamappa have separately publishing a number of papers demonstrating the detection of a several drug molecules graphene modified glassy carbon electrodes, including the detection of the anti-migraine drug rizatriptan benzoate.[202,203] In 2014 Seetharamappa reported the use of differential pulse voltammetry to measure the oxidation of the drug using glassy carbon electrode modified with electrochemically reduced graphene oxide. Using this system a linear response over the range of 0.1–40 nM and a limit of detectability of 57.1 nM was obtained.[202] Also in 2014 Jain and Pandey investigated the enhancement effect on the detection of rizatriptan by a graphene modified GCE due to the presence of the cationic surfactant cetyltrimethyl ammonium bromide (CTAB) in the sample solution. The anodic peak was found to increase in the presence of CTAB, up to a concentration of 0.12%, at greater concentrations the formation of micelles resulted in a decrease in the current.[203] In this sensor an improved limit of detectability of 36.3 nM was obtained and this improved electrochemical response may be attributed to the presence of the long hydrophobic chain in CTAB which act to accumulation the analyte at the electrode surface. This approach has also been used to sense caffeine. [208]

In general, the selective electrochemical detection of different drugs is typically poor as it is hindered by the overlap of anodic peaks. This limitation has begun to be addressed through the preparation of modified graphene coatings on the working electrode and by the use of screen printed electrodes with either molecular imprinted film[204] or graphene modified carbon ink.[195] In particular, screen printed electrodes have emerged as a cost effective solution. In one recent example a screen printed electrode comprising a two distinct molecularly imprinted films has allowed simultaneous detection of methcaninone and cathinone.[204] The limits of detection of for the drugs were found to be 20.2 pM and 59.6 pM respectively and minimal cross-talk was between the two molecularly imprinted films was observed. In addition, using graphene modified carbon ink, the pesticides isoproturon and carbendazim could be simultaneously detected with square wave voltammetry peaks at 0.78 V and 1.08 V respectively, see Figure 23.[195]

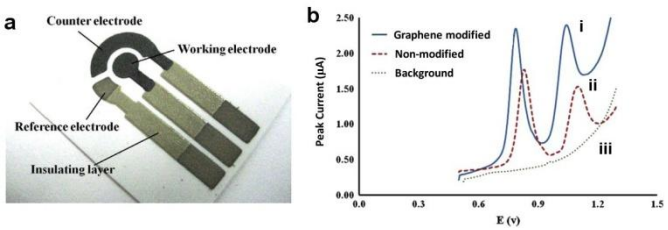

Fig. 24 (a) Schematic of a standard screen print electrode (b) Representative square wave stripping voltammetric traces for mixed solution isoproturon and carbendazim pesticides (5.0 mg/L each) for (i) graphene-modified carbon sensor, and (ii) non-modified carbon sensor, compared to (iii) the background. Reprinted with permission from Ref.[195] Copyright (2014) Elsevier.

Modified Graphene/GCEs have demonstrated improved enhancement of sensitivity for single, and multiple drug molecule detection. A graphene/GCE modified with $NiFe_2O_4$ nanoparticles was recently shown to facilitate simultaneous detection enhancement of tramadol and acetaminophen; two analgesic drugs. Impedance measurements showed that the electron transfer resistance decreased in the presence of the nanoparticles. This is attributed to the increase of surface area, the conductivity of the nanoparticles and the added electroactivity arising due to the interaction of the molecules at the nanoparticle surface.[198]

Graphene sensing of biomolecules

Graphene containing sensors have been used to detect a wide range of biomolecules, including; target DNA strands,[210,211] norepinephrine,[212] glucose,[213] glutamate,[213,214] uric acid,[215,216] ascorbic acid[215,216] and L-cysteine.[217] While, the greatest focus has been directed towards the detection of dopamine.[215,216,218–221] Xing *et al.* demonstrated the use of graphene oxide as a platform for to detect target DNA through the use of a FRET based process.[210] The same group used this approach to detect K^+ (Figure 22). Fluorescein (FAM)-labelled single stranded DNA was immobilized onto a sheet of graphene oxide where the emission is quenched. In the presence of the complementary strand of DNA binding occurs preventing the interaction of the fluorescently labelled sequence with the graphene oxide. The cationic conjugated polymer, PFP, is then added, which binds to the newly formed double stranded DNA, inducing FRET and giving a fluorescent signal. This detection is sensitive to single mismatches. In the presence of two or more mismatches the sequence remains at the GO surface. This is another nice example of a DNA sensor as its limit of detection was determined to be 40 pM with a fluorescence turn on ratio of 7.60 in the presence of GO, as opposed to a ratio of 1.20 from traditional PFP systems.

Whilst taking advantage of the inherent properties of graphene, increasingly biosensors are being developed that exploit 'synergistic' electrocatalytic activity displayed by graphene in the presence of a wide range of substances including gold nanoparticles,[219] Fe_3O_4,[216] nickel hydroxide[215] and cobalt phthalocyanine.[217] As already noted in previous examples this synergetic effect may be attributed to additional surface area provided by the presence of nanoparticles, increased affinity for the analyte or improved redox properties conferred to the sensor. However, it should be noted that simultaneous detection typcailly occurs with less sensitivity than dedicated sensors.

Wu *et al.* developed an Fe_3O_4-NH_2@Graphene/GCE system to detect and quantify ascorbic acid (AA), dopamine (DA) and uric acid (UA) simultaneously.[216] The Fe_3O_4-NH_2@graphene electrode exhibits enhanced electrochemical catalytic oxidation of AA, DA and UA in comparison to the simple graphene-GCE, *see* Figure 25a. In addition it facilitated the resolution of the overlapping anodic peaks with a linear response *see* Figure 25b.[216] The authors note the presence of a mesoporous structure

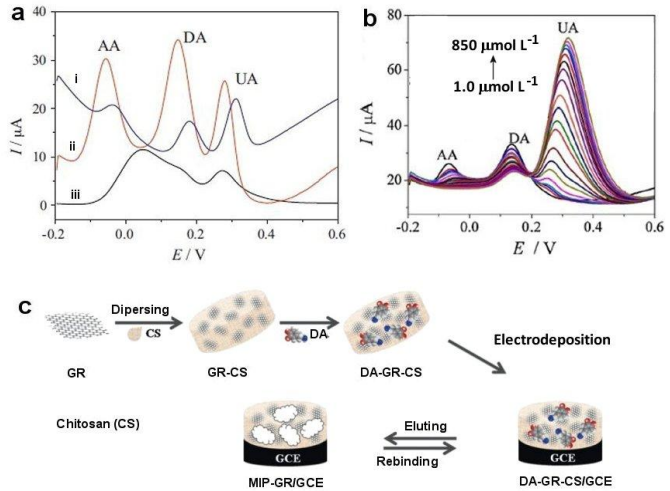

Fig. 25 (a) Differential pulse voltammograms (DPV) for AA, DA and UA at (i) bare GCE, (ii) GS/GCE and (iii) Fe_3O_4-NH_2@GS/GCE (b) Fe_3O_4-NH2@GS modified electrode in PBS (pH 7.0) containing 100 μmol L^{-1} AA, 5.0 μmol L^{-1} DA and different concentrations of UA. (c) Preparation of MIPs-GR/GCE and its recognition for DA. (a-b) Reprinted with permission from Ref.[216] (c) Adapted from ref [220]. Copyright (2012 & 2013) Elsevier.

at the surface of the magnetic nanoparticles with a pore size of 12 nm which contributes to enhanced surface area.

Excellent dopamine sensitivity was demonstrated by Liu *et al.* using a molecularly imprin ted polymer (MIP) electrochemical sensor based on an graphene-chitosan composite.[220] This involved synthesising a dopamine-graphene-chitosan complex before electrodeposing it onto a glassy carbon electrode. The dopamine was then eluted off the sensor, see Figure 25c. The selectivity to dopamine was high, with the MIP sensors showing little change in the peak current ratio (I/I_0 where I_0 is the current response to 1.0×10^{-6} M dopamine and I is the current response when various concentrations of co-existing species are present), *see* Table 2.[220]
Overall, it can be seen that graphene containing sensors can be used on a wide range of biomolecules with great selectivity and sensitivity. The most recent focus has been on the development of sensors that exhibit the 'synergistic' effect and can be utilized in the simultaneous determination of multiple biomolecules, or the development of sensors that can target single molecules down to low/ sub nM levels.

Carbon Nanomaterial Safety Considerations

This review has highlighted how the unique and advantageous properties of carbon nanomaterials make them ideal platforms for sensing. However, significant concerns exist in relation to the safety of nanosized materials. [222, 223, 224] Depending on the nature of exposure, nanoparticles may enter the body through the lungs, the skin and the gut.[225] Thus the explosion in cell permeable engineered materials raises important questions about cell interactions, including the mechanism of entry, the final destination in the cell and the possible adverse effects.[226] Consequently, information on the risk posed by exposure of humans and/or the environment to nanomaterials has been the subject of sustained discussion and investigation which aims to put in place regulations that minimize the risk of nanomaterials.[227]

In particular, the high aspect ratio of CNTs has led to their comparison with harmful fibrous materials such as asbestos.[228, 229, 230] A number of reviews have considered physico-chemical properties of CNTs that contribute to toxicity. [231, 232, 233] A large number of studies have considered the toxicity of CNTs to biological function by considering cellular uptake[234] and cell death.[230, 235] The impact of CNTs on workplace safety and environmental health has also been reported.[236, 229] These and numerous other studies have revealed CNTs to have summarize negative effects on living organisms. This has been attributed to factors such as the size of the nanoparticles, the presence of toxic residual catalyst particles and the presence of surface bound carbonaceous fragments that can act as ROS species.[237] With this information to hand we can now begin to describe the conditions under which it is safe to use CNT materials and this was recently described in a review on the safe clinical use of carbon nanotubes in the area of innovative biomaterials by Iijima and co-workers.[238]

However, some CNMs have demonstrated less toxicity. CNHs and nanodiamonds have been found to demonstrate low or no toxicity.[60, 239] However, CNOs have been found to exhibit

Table 2: Table summarising the detection of analytes by Graphene based sensors. (LR= linear range, LOD = limit of detection)

Graphene Sensor Type	Detection Type	Target Cation	LR	LOD	Ref.
Graphene Oxide Sheet/fluorescent tagged ssDNA	Fluorescence	ssDNA	0.05-20 nM	0.04 nM	210
Cu_2O/Graphene/GCE	Current	Dopamine	0.1-10 μM	10 nM	218
Multi layers of Reduced graphene oxide/AuNPs on GCE	Current	Dopamine Uric Acid	1-60 μM 10-120 μM	20 nM 270 nM	219
Porphyrin fuctionalized graphene/GCE	Current	Dopamine	0.1-1 μM	22 nM	221
Molecularly imprinted polymer-Graphene/GCE	Current	Dopamine	1-100 nM; 0.1-100 μM	10 pM	220
Graphene Oxide-cobalt phthalocyanine/GCE	Current	L-cysteine	0.01-200 μM	5 nM	217
Graphene modified palladium/GCE	Current	Norepinephrine	0.5-500 μM	67.4 nM	212
Fe_3O_4@Graohene Sheets/GCE	Current	Dopamine Uric Acid Ascorbic Acid	0.2-38 μM 1-850 μM 5-1600 μM	126 nM 56 nM 74 nM	216
Graphene/nickel hydroxide/GCE	Current	Dopamine Uric Acid Ascorbic Acid	0.44-3.3 μM 2-15 μM 150-300 μM	120 nM 460 nM 30 μM	215

size dependent toxicity with smaller CNOs being less toxic.[240] [241] Graphene is now the subject of investigation[242] and it is felt that lessons may be learnt from the study of CNTs.[243] Such studies are is particularly relevant due to the high number of sensors being developed from this material. As yet there is limited data on the toxicity of Cdots but indications are that they exhibit low toxicity.[244] These considerations may act to influence the choice of CNM for sensor application.

Conclusions and Outlook

Carbon nanomaterials have emerged as an excellent sensing platform. These sensors and biosensors are notable for the high surface area, which allow many simultaneous detection events. CNMs are truly distinguished from other nanomaterials by their diverse and robust intrinsic optical and electronic properties. The versatility of these materials is demonstrated by the use of carbon dots, carbon nanotubes and graphene as either discrete molecular-like sensors or as assemblies and composites which can be integrated into devices. This continues to stimulate advances in the area of sensing and biosensing with an ever growing variety of systems being developed year on year.

In this review we have considered recent developments in the area of CNM sensors. We have described examples of CNM fluorescence based sensing by CNDs, Cdots, CNTs and GO materials. In particular the combination of biocompatibility and NIR luminescence of semiconducting nanotubes holds great promise for *in vivo* sensing. Other exciting developments include the use of carbon nanomaterial platforms for *in vitro* sensing of cellular processes under exposure to different external stimuli. Going forward, it is expected that Cdots will find greater application for *in vivo* sensing. The combination of supramolecular chemistry, and aptamer based approaches with CNMs optical properties offers great potential for selective optical-based sensing in the presence of interferents, which can be enhanced by amplification of CNMs sensor arrays.

CNM based electrochemical sensors are considered as the second sensing pillar. The electroactivity of CNO, CND, CNTs and graphene have been extensively demonstrated for sensing, where their increased conductivity and surface area are readily exploited. Furthermore, the promise of cheap disposable sensors has been aided by developments in screen printed CNM-based electrodes using carbon 'inks'. However, a note of caution is required as a recent study by Ma *et al.* has shown that CNTs activity is greatly varied due to the adsorption of carbonaceous fragments, which are a by-product of acid treatments.[245] Significantly, the removal of the carbonaceous fragments resulted in a decrease in the electrocatalytic oxidation of ascorbic acid by the CNT electrode. This result suggests that further research is required to understand the contribution of these impurities to electrochemical CNM sensors.

Going forward it is clear that realising the potential of CNMs for routine sensing, and to see their widespread integration into sensing devices, necessitates the availability of sufficient quantities of pure and safe materials. This requires continued efforts in the areas of size selective synthesis, purification and separation of CNM species and consensus regarding the safety considerations. With progress on these fronts the future of carbon nanomaterial sensors is very bright indeed.

Acknowledgements

FB and SJQ are grateful to University College Dublin for funding and SG is grateful to the Istituto Italiano di Tecnologia (IIT) for funding. SB would like to acknowledge the financial support of Irish Research Council grant no. GOIPG/2013/1110.

Notes and references

[a]*School of Chemistry, University College Dublin, Dublin 4, Ireland. Tel: +353-1-716-2407; E-mail: susan.quinn@ucd.ie*
[b] *Istituto Italiano di Tecnologia (IIT), Nano Carbon Materials, Nanophysics Department, Via Morego 30, 16163 Genova, Italy.*

1. K. L. Kelly, E. Coronado, L. L. Zhao, and G. C. Schatz, *J. Phys. Chem. B*, 2003, **107**, 668–677.
2. K. Saha, S. S. Agasti, C. Kim, X. Li, and V. M. Rotello, *Chem. Rev.*, 2012, **112**, 2739–79.
3. G. Konvalina and H. Haick, *Acc. Chem. Res.*, 2014, **47**, 66–76.
4. B. Valeur and I. Leray, *Coord. Chem. Rev.*, 2000, **205**, 3–40.
5. B. M. S. Dresselhaus and M. Terrones, *Proc. IEEE*, 2013, **101**, 1522–1535.
6. H. W. Kroto, J. R. Heath, S. C. O'Brien, *Nature*, 1985, **318**, 162–163.
7. S. Iijima, *Nature*, 1991, **354**, 56–58.
8. S. Iijima and I. Toshhinari, *Nature*, 1993, **363**, 603–605.
9. V. L. Kuznetsov, A. L. Chuvilin, Y. V. Butenko, I. Y. Mal'kov, and V. M. Titov, *Chem. Phys. Lett.*, 1994, **222**, 343–348.
10. S. Iijima and M. Yudasaka, *Chem. Phys. Lett.*, 1999, **309**, 165–170.
11. V. V. Danilenko, *Phys. Solid State*, 2004, **46**, 595–599.
12. W. Yang, K. R. Ratinac, S. P. Ringer, P. Thordarson, J. J. Gooding, and F. Braet, *Angew. Chem. Int. Ed. Engl.*, 2010, **49**, 2114–2138.
13. S. Zhu and G. Xu, *Nanoscale*, 2010, **2**, 2538–2349.
14. D. Jariwala, V. K. Sangwan, L. J. Lauhon, T. J. Marks, and M. C. Hersam, *Chem. Soc. Rev.*, 2013, **42**, 2824–2860.
15. D. Ugarte, *Nature*, 1992, **359**, 707–709.
16. A. Palkar, A. Kumbhar, A. J. Athans, and L. Echegoyen, *Chem. Mater.*, 2008, **20**, 1685–1687.
17. C. T. Cioffi, A. Palkar, F. Melin, A. Kumbhar, L. Echegoyen, M. Melle-Franco, F. Zerbetto, G. M. A. Rahman, C. Ehli, V. Sgobba, D. M. Guldi, and M. Prato, *Chem. A Eur. J.*, 2009, **15**, 4419–4427.
18. J. Luszczyn, M. E. Plonska-Brzezinska, A. Palkar, A. T. Dubis, A. Simionescu, D. T. Simionescu, B. Kalska-Szostko, K. Winkler, and L. Echegoyen, *Chem. A Eur. J.*, 2010, **16**, 4870–4880.
19. J. Breczko, M. E. Plonska-Brzezinska, and L. Echegoyen, *Electrochim. Acta*, 2012, **72**, 61–67.
20. V. N. Mochalin, O. Shenderova, D. Ho, and Y. Gogotsi, *Nat. Nanotechnol.*, 2012, **7**, 11–23.
21. L. Tang, C. Tsai, W. W. Gerberich, L. Kruckeberg, and D. R. Kania, *Biomaterials*, 1995, **16**, 483–488.

22. A. M. Schrand, H. Huang, C. Carlson, J. J. Schlager, E. Omacr Sawa, S. M. Hussain, and L. Dai, *J. Phys. Chem. B*, 2007, **111**, 2–7.
23. V. V. Danilenko, *Phys. Solid State*, 2004, **46**, 595–599.
24. R. Schirhagl, K. Chang, M. Loretz, and C. L. Degen, *Annu. Rev. Phys. Chem.*, 2014, **65**, 83–105.
25. I. I. Vlasov, A. a Shiryaev, T. Rendler, S. Steinert, S.-Y. Lee, D. Antonov, M. Vörös, F. Jelezko, A. V Fisenko, L. F. Semjonova, J. Biskupek, U. Kaiser, O. I. Lebedev, I. Sildos, P. R. Hemmer, V. I. Konov, A. Gali, and J. Wrachtrup, *Nat. Nanotechnol.*, 2014, **9**, 54–58.
26. Y. Sun, B. Zhou, and Y. Lin, *J. Am. Chem. Soc.*, 2006, **128**, 7756–7757.
27. H. Liu, T. Ye, and C. Mao, *Angew. Chem. Int. Ed. Engl.*, 2007, **46**, 6473–6475.
28. L. Zhu, Y. Yin, C.-F. Wang, and S. Chen, *J. Mater. Chem. C*, 2013, **1**, 4925-4932.
29. Y. Guo, Z. Wang, H. Shao, and X. Jiang, *Carbon N. Y.*, 2013, **52**, 583–589.
30. X. Gao, C. Ding, A. Zhu, and Y. Tian, *Anal. Chem.*, 2014, **86**, 7071–7078.
31. Y. Liu, N. Xiao, N. Gong, H. Wang, X. Shi, W. Gu, and L. Ye, *Carbon N. Y.*, 2014, **68**, 258–264.
32. X. W. Tan, A. N. B. Romainor, S. F. Chin, and S. M. Ng, *J. Anal. Appl. Pyrolysis*, 2014, **105**, 157–165.
33. X. Qin, W. Lu, A. M. Asiri, A. O. Al-Youbi, and X. Sun, *Sensors Actuators B Chem.*, 2013, **184**, 156–162.
34. X. Yang, Y. Zhuo, S. Zhu, Y. Luo, Y. Feng, and Y. Dou, *Biosens. Bioelectron.*, 2014, **60**, 292–298.
35. Y. Liu, Y. Zhao, and Y. Zhang, *Sensors Actuators B Chem.*, 2014, **196**, 647–652.
36. Y. Dong, R. Wang, H. Li, J. Shao, Y. Chi, X. Lin, and G. Chen, *Carbon N. Y.*, 2012, **50**, 2810–2815.
37. W. Wei, C. Xu, J. Ren, B. Xu, and X. Qu, *Chem. Commun. (Camb).*, 2012, **48**, 1284–1286.
38. Z. Lin, W. Xue, H. Chen, and J. Lin, *Anal. Chem.*, 2011, **83**, 8245–8251.
39. S. N. Baker and G. a Baker, *Angew. Chem. Int. Ed. Engl.*, 2010, **49**, 6726–6744.
40. H. Li, Z. Kang, Y. Liu, and S.-T. Lee, *J. Mater. Chem.*, 2012, **22**, 24230-24253.
41. C. Ding, A. Zhu, and Y. Tian, *Acc. Chem. Res.*, 2014, **47**, 20–30.
42. K. S. Novoselov, a K. Geim, S. V Morozov, D. Jiang, Y. Zhang, S. V Dubonos, I. V Grigorieva, and a a Firsov, *Science*, 2004, **306**, 666–669.
43. A. K. Geim and K. S. Novoselov, *Nat. Mater.*, 2007, **6**, 183–191.
44. M. J. Allen, V. C. Tung, and R. B. Kaner, *Chem. Rev.*, 2010, **110**, 132–145.
45. J. N. Coleman, *Acc. Chem. Res.*, 2013, **46**, 14–22.
46. K. R. Paton, E. Varrla, C. Backes, R. J. Smith, U. Khan, A. O'Neill, C. Boland, M. Lotya, O. M. Istrate, P. King, T. Higgins, S. Barwich, P. May, P. Puczkarski, I. Ahmed, M. Moebius, H. Pettersson, E. Long, J. Coelho, S. E. O'Brien, E. K. McGuire, B. M. Sanchez, G. S. Duesberg, N. McEvoy, T. J. Pennycook, C. Downing, A. Crossley, V. Nicolosi, and J. N. Coleman, *Nat. Mater.*, 2014, **13**, 624–630.
47. C.-T. Chien, S.-S. Li, W.-J. Lai, Y.-C. Yeh, H.-A. Chen, I.-S. Chen, L.-C. Chen, K.-H. Chen, T. Nemoto, S. Isoda, M. Chen, T. Fujita, G. Eda, H. Yamaguchi, M. Chhowalla, and C.-W. Chen, *Angew. Chemie Int. Ed.*, 2012, **51**, 6662–6666.
48. V. Georgakilas, M. Otyepka, A. B. Bourlinos, V. Chandra, N. Kim, K. C. Kemp, P. Hobza, R. Zboril, and K. S. Kim, *Chem. Rev.*, 2012, **112**, 6156–214.
49. S. Eigler and A. Hirsch, *Angew. Chem. Int. Ed. Engl.*, 2014, **53**, 7720–7738.
50. B. L. Allen, P. D. Kichambare, and a. Star, *Adv. Mater.*, 2007, **19**, 1439–1451.
51. D. R. Kauffman and A. Star, *Angew. Chem. Int. Ed. Engl.*, 2008, **47**, 6550–6570.
52. S. Kruss, A. J. Hilmer, J. Zhang, N. F. Reuel, B. Mu, and M. S. Strano, *Adv. Drug Deliv. Rev.*, 2013, **65**, 1933–1950.
53. C. Li and G. Shi, *J. Photochem. Photobiol. C Photochem. Rev.*, 2014, **19**, 20–34.
54. J. V. & R. B. D. S. Bethune, C. H. Kiang, M. S. de Vries, G. Gorman, R. Savoy, *Nature*, 1993, **363**, 605–607.
55. C.-M. Yang, H. Noguchi, K. Murata, M. Yudasaka, a. Hashimoto, S. Iijima, and K. Kaneko, *Adv. Mater.*, 2005, **17**, 866–870.
56. T. Yamaguchi, S. Bandow, and S. Iijima, *Chem. Phys. Lett.*, 2004, **389**, 181–185.
57. H. Dai, *Acc. Chem. Res.*, 2002, **35**, 1035–1044.
58. A. Dupuis, *Prog. Mater. Sci.*, 2005, **50**, 929–961.
59. H. Hu, B. Zhao, M. Itkis, and R. Haddon, *J. Phys. Chem. B*, 2003, **107**, 13838–13842.
60. J. Miyawaki, M. Yudasaka, T. Azami, Y. Kubo, and S. Iijima, *ACS Nano*, 2008, **2**, 213–226.
61. K. Flavin, I. Kopf, E. Del Canto, C. Navio, and S. Giordani, *J. Mater. Chem.*, 2011, **21**, 17881–17887.
62. Z. Wu, R. F. Hamilton, Z. Wang, A. Holian, and S. Mitra, *Carbon N. Y.*, 2014, **68**, 678–686.
63. M. C. Hersam, *Nat. Nanotechnol.*, 2008, **3**, 387–394.
64. S. Ghosh, S. M. Bachilo, and R. B. Weisman, *Nat. Nanotechnol.*, 2010, **5**, 443–450.
65. B. S. Flavel, K. E. Moore, M. Pfohl, M. M. Kappes, and F. Hennrich, *ACS Nano*, 2014, **8**, 1817–1826.
66. J. Fagan, M. Becker, J. Chun, and P. Nie, *Langmuir*, 2008, **24**, 13880–13889.
67. U. Khan, A. O'Neill, H. Porwal, P. May, K. Nawaz, and J. N. Coleman, *Carbon N. Y.*, 2012, **50**, 470–475.
68. C. a. Dyke and J. M. Tour, *J. Phys. Chem. A*, 2004, **108**, 11151–11159.
69. V. Georgakilas and K. Kordatos, *J. Am. Chem. Soc.*, 2002, **124**, 760–761.
70. A. Hirsch, *Angew. Chem. Int. Ed. Engl.*, 2002, **41**, 1853–1859.
71. P. Singh, S. Campidelli, S. Giordani, D. Bonifazi, A. Bianco, and M. Prato, *Chem. Soc. Rev.*, 2009, **38**, 2214–2230.
72. K. E. Sapsford, W. R. Algar, L. Berti, K. B. Gemmill, B. J. Casey, E. Oh, M. H. Stewart, and I. L. Medintz, *Chem. Rev.*, 2013, **113**, 1904–2074.
73. V. Biju, *Chem. Soc. Rev.*, 2014, **43**, 744–764.
74. R. J. Chen, Y. Zhang, D. Wang, and H. Dai, *J. Am. Chem. Soc.*, 2001, **123**, 3838–3839.
75. Y. Zhao and J. Stoddart, *Acc. Chem. Res.*, 2009, **42**, 1161–1171.

76. I. Union, O. F. Pure, and A. Chemistry, 1991, **63**, 1247–1250.
77. E. M. Nolan and S. J. Lippard, *Chem. Rev.*, 2008, **108**, 3443–3480.
78. F. Zahir, S. J. Rizwi, S. K. Haq, and R. H. Khan, *Environ. Toxicol. Pharmacol.*, 2005, **20**, 351–360.
79. L. Xu, S. Liang, and L. Gan, *Org. Chem. Front.*, 2014, **1**, 652–656.
80. L. Lin and J. Shih, *J. Chinese Chem. Soc.*, 2011, **58**, 228–235.
81. W. Zhilei, L. Zaijun, S. Xiulan, F. Yinjun, and L. Junkang, *Biosens. Bioelectron.*, 2010, **25**, 1434–1438.
82. C.-W. Chuang and J.-S. Shih, *Sensors Actuators B Chem.*, 2001, **81**, 1–8.
83. H. Wu, S. Fan, X. Jin, H. Zhang, H. Chen, Z. Dai, and X. Zou, *Anal. Chem.*, 2014, **86**, 6285–6290.
84. H.-B. Lin and J.-S. Shih, *Sensors Actuators B Chem.*, 2003, **92**, 243–254.
85. J.-S. Shih, Y.-C. Chao, M.-F. Sung, G.-J. Gau, and C.-S. Chiou, *Sensors Actuators B Chem.*, 2001, **76**, 347–353.
86. S. Afreen, K. Muthoosamy, S. Manickam, and U. Hashim, *Biosens. Bioelectron.*, 2015, **63**, 354–64.
87. A. Krueger and D. Lang, *Adv. Funct. Mater.*, 2012, **22**, 890–906.
88. A. Gruber, A. Dräbenstedt, C. Tietz, L. Fleury, J. Wrachtrup, and C. von Borczyskowski, *Science*, 1997, **276**, 2012–2014.
89. P. Neumann, I. Jakobi, F. Dolde, C. Burk, R. Reuter, G. Waldherr, J. Honert, T. Wolf, A. Brunner, and J. H. Shim, *Nano Lett.*, 2013, **13**, 2738–2742.
90. G. Kucsko, P. C. Maurer, N. Y. Yao, M. Kubo, H. J. Noh, P. K. Lo, H. Park, and M. D. Lukin, *Nature*, 2013, **500**, 54–8.
91. A. Ermakova, G. Pramanik, J.-M. Cai, G. Algara-Siller, U. Kaiser, T. Weil, Y.-K. Tzeng, H. C. Chang, L. P. McGuinness, M. B. Plenio, B. Naydenov, and F. Jelezko, *Nano Lett.*, 2013, **13**, 3305–3309.
92. J. R. Maze, P. L. Stanwix, J. S. Hodges, S. Hong, J. M. Taylor, P. Cappellaro, L. Jiang, M. V. G. Dutt, E. Togan, a S. Zibrov, A. Yacoby, R. L. Walsworth, and M. D. Lukin, *Nature*, 2008, **455**, 644–647.
93. S. Kaufmann, D. A. Simpson, L. T. Hall, V. Perunicic, P. Senn, S. Steinert, L. P. McGuinness, B. C. Johnson, T. Ohshima, F. Caruso, J. Wrachtrup, R. E. Scholten, P. Mulvaney, and L. Hollenberg, *Proc. Natl. Acad. Sci. U. S. A.*, 2013, **110**, 10894–10898.
94. R. K. Ahmad, A. C. Parada, S. Hudziak, A. Chaudhary, and R. B. Jackman, *Appl. Phys. Lett.*, 2010, **97**, 093103.
95. J. Wang and X. Qu, *Nanoscale*, 2013, **5**, 3589–3600.
96. Y. Guo, L. Zhang, S. Zhang, Y. Yang, X. Chen, and M. Zhang, *Biosens. Bioelectron.*, 2015, **63**, 61–71.
97. H. M. R. Gonçalves, A. J. Duarte, and J. C. G. Esteves da Silva, *Biosens. Bioelectron.*, 2010, **26**, 1302–1306.
98. R. Liu, H. Li, W. Kong, J. Liu, Y. Liu, C. Tong, X. Zhang, and Z. Kang, *Mater. Res. Bull.*, 2013, **48**, 2529–2534.
99. F. Yan, Y. Zou, M. Wang, X. Mu, N. Yang, and L. Chen, *Sensors Actuators B Chem.*, 2014, **192**, 488–495.
100. R. Zhang and W. Chen, *Biosens. Bioelectron.*, 2014, **55**, 83–90.
101. S. Zhu, Q. Meng, L. Wang, J. Zhang, Y. Song, H. Jin, K. Zhang, H. Sun, H. Wang, and B. Yang, *Angew. Chem. Int. Ed. Engl.*, 2013, **52**, 3953–3957.
102. S. Qu, H. Chen, X. Zheng, J. Cao, and X. Liu, *Nanoscale*, 2013, **5**, 5514–5518.
103. A. Zhao, C. Zhao, M. Li, J. Ren, and X. Qu, *Anal. Chim. Acta*, 2014, **809**, 128–133.
104. Y.-L. Zhang, L. Wang, H.-C. Zhang, Y. Liu, H.-Y. Wang, Z.-H. Kang, and S.-T. Lee, *RSC Adv.*, 2013, **3**, 3733–3738.
105. Z. Zhang, Y. Shi, Y. Pan, X. Cheng, L. Zhang, J. Chen, M.-J. Li, and C. Yi, *J. Mater. Chem. B*, 2014, **2**, 5020–5027.
106. Y. Zou, F. Yan, L. Dai, Y. Luo, Y. Fu, N. Yang, J. Wun, and L. Chen, *Carbon N. Y.*, 2014, **77**, 1148–1156.
107. M. Algarra, B. B. Campos, K. Radotić, D. Mutavdžić, T. Bandosz, J. Jiménez-Jiménez, E. Rodriguez-Castellón, and J. C. G. Esteves da Silva, *J. Mater. Chem. A*, 2014, **2**, 8342–8351.
108. L. Shen, M. Chen, L. Hu, X. Chen, and J. Wang, *Langmuir*, 2013, **29**, 16135–16140.
109. X. Li, S. Zhang, S. a Kulinich, Y. Liu, and H. Zeng, *Sci. Rep.*, 2014, **4**, 4976.
110. S. Zhang, Q. Wang, G. Tian, and H. Ge, *Mater. Lett.*, 2014, **115**, 233–236.
111. F. Du, F. Zeng, Y. Ming, and S. Wu, *Microchim. Acta*, 2013, **180**, 453–460.
112. Z. Huang, F. Lin, M. Hu, C. Li, T. Xu, C. Chen, and X. Guo, *J. Lumin.*, 2014, **151**, 100–105.
113. L. Zhou, Y. Lin, Z. Huang, J. Ren, and X. Qu, *Chem. Commun. (Camb).*, 2012, **48**, 1147–1149.
114. X. Yang, Y. Luo, S. Zhu, Y. Feng, Y. Zhuo, and Y. Dou, *Biosens. Bioelectron.*, 2014, **56**, 6–11.
115. Z. Qian, X. Shan, L. Chai, J. Ma, J. Chen, and H. Feng, *ACS Appl. Mater. Interfaces*, 2014, **6**, 6797–6805.
116. Y. Song, S. Zhu, S. Xiang, X. Zhao, J. Zhang, H. Zhang, Y. Fu, and B. Yang, *Nanoscale*, 2014, **6**, 4676–4682.
117. A. Cayuela, M. L. Soriano, and M. Valcárcel, *Anal. Chim. Acta*, 2013, **804**, 246–251.
118. M. P. Sk and A. Chattopadhyay, *RSC Adv.*, 2014, **4**, 31994.
119. J. Niu and H. Gao, *J. Lumin.*, 2014, **149**, 159–162.
120. S. Yang, J. Liang, S. Luo, C. Liu, and Y. Tang, *Anal. Chim. Acta*, 2013, **85**, 7720–7725.
121. J. Wei, J. Ren, J. Liu, X. Meng, X. Ren, Z. Chen, and F. Tang, *Biosens. Bioelectron.*, 2014, **52**, 304–309.
122. Y. Shi, Y. Pan, H. Zhang, Z. Zhang, M.-J. Li, C. Yi, and M. Yang, *Biosens. Bioelectron.*, 2014, **56**, 39–45.
123. A. Zhu, Z. Luo, C. Ding, B. Li, S. Zhou, R. Wang, and Y. Tian, *Analyst*, 2014, **139**, 1945–1952.
124. J. Zong, X. Yang, A. Trinchi, S. Hardin, I. Cole, Y. Zhu, C. Li, T. Muster, and G. Wei, *Biosens. Bioelectron.*, 2014, **51**, 330–335.
125. X.-M. Wei, Y. Xu, Y.-H. Li, X.-B. Yin, and X.-W. He, *RSC Adv.*, 2014, **4**, 44504–44508.
126. Y. Wang, S. Wang, S. Ge, S. Wang, M. Yan, D. Zang, and J. Yu, *Anal. Methods*, 2013, **5**, 1328–1336.
127. W. Bai, H. Zheng, Y. Long, X. Mao, M. Gao, and L. Zhang, *Anal. Sci.*, 2011, **27**, 243–246.
128. M. Zheng, Z. Xie, D. Qu, D. Li, P. Du, X. Jing, and Z. Sun, 2013.
129. F. Lin, D. Pei, W. He, Z. Huang, Y. Huang, and X. Guo, *J. Mater. Chem.*, 2012, **22**, 11801–11807.
130. K. M. Tripathi, A. K. Sonker, S. K. Sonkar, and S. Sarkar, *RSC Adv.*, 2014, **4**, 30100–30107.
131. S. Maiti, K. Das, and P. K. Das, *Chem. Commun. (Camb).*, 2013, **49**, 8851–8853.

132. S. Hu, Q. Huang, Y. Lin, C. Wei, H. Zhang, W. Zhang, Z. Guo, X. Bao, J. Shi, and A. Hao, *Electrochim. Acta*, 2014, **130**, 805–809.
133. W. Deng, F. Liu, S. Ge, J. Yu, M. Yan, and X. Song, *Analyst*, 2014, **139**, 1713–1720.
134. P. Shen and Y. Xia, *Anal. Chem.*, 2014, **86**, 5323–5329.
135. X. Shan, L. Chai, J. Ma, Z. Qian, J. Chen, and H. Feng, *Analyst*, 2014, **139**, 2322–2325.
136. C. Yu, X. Li, F. Zeng, F. Zheng, and S. Wu, *Chem. Commun. (Camb).*, 2013, **49**, 403–405.
137. S. M. Khamis, R. a. Jones, a. T. C. Johnson, G. Preti, J. Kwak, and a. Gelperin, *AIP Adv.*, 2012, **2**, 022110.
138. N. J. Kybert, M. B. Lerner, J. S. Yodh, G. Preti, and a T. C. Johnson, *ACS Nano*, 2013, **7**, 2800–2807.
139. J.-H. Kim, D. A. Heller, H. Jin, P. W. Barone, C. Song, J. Zhang, L. J. Trudel, G. N. Wogan, S. R. Tannenbaum, and M. S. Strano, *Nat Chem*, 2009, **1**, 473–481.
140. D. Heller, G. Pratt, and J. Zhang, *Proc. Natl. Acad. Sci. U. S. A.*, 2011, **108**, 8544–8549.
141. K. Balasubramanian and M. Burghard, *Anal. Bioanal. Chem.*, 2006, **385**, 452–68.
142. J. Wang, *Electroanalysis*, 2005, **17**, 7–14.
143. S. K. Vashist, D. Zheng, K. Al-Rubeaan, J. H. T. Luong, and F.-S. Sheu, *Biotechnol. Adv.*, 2011, **29**, 169–88.
144. P. J. Britto, K. S. V. Santhanam, and P. M. Ajayan, *Bioelectrochemistry Bioenerg.*, 1996, **41**, 121–125.
145. K. Besteman, J.-O. Lee, F. G. M. Wiertz, H. a. Heering, and C. Dekker, *Nano Lett.*, 2003, **3**, 727–730.
146. G. Zhu, X. Zhang, P. Gai, X. Zhang, and J. Chen, *Nanoscale*, 2012, **4**, 5703–5709.
147. L. Gu, Y. Liang, T. Zhou, X. Tang, and G. Shi, *Anal. Methods*, 2012, **4**, 492–495.
148. B. Shah, T. Lafleur, and A. Chen, *Faraday Discuss.*, 2013, **164**, 135–146.
149. L. Asturias-Arribas, M. A. Alonso-Lomillo, O. Domínguez-Renedo, and M. J. Arcos-Martínez, *Anal. Chim. Acta*, 2014, **834**, 30–36.
150. S. Antwi-Boampong, K. S. Mani, J. Carlan, and J. J. BelBruno, *J. Mol. Recognit.*, 2014, **27**, 57–63.
151. P. W. Barone, S. Baik, D. a Heller, and M. S. Strano, *Nat. Mater.*, 2005, **4**, 86–92.
152. K. Yum, J.-H. Ahn, T. P. McNicholas, P. W. Barone, B. Mu, J.-H. Kim, R. M. Jain, and M. S. Strano, *ACS Nano*, 2012, **6**, 819–30.
153. D. A. Heller, H. Jin, B. M. Martinez, D. Patel, B. M. Miller, T. Yeung, P. V Jena, C. Höbartner, T. Ha, S. K. Silverman, and M. S. Strano, *Nat. Nanotechnol.*, 2009, **4**, 114–120.
154. L. Zhan, L. Peng, Y. Yu, S. J. Zhen, and C. Z. Huang, *Analyst*, 2012, **137**, 4968–4973.
155. J.-H. Ahn, J.-H. Kim, N. F. Reuel, P. W. Barone, A. a Boghossian, J. Zhang, H. Yoon, A. C. Chang, A. J. Hilmer, and M. S. Strano, *Nano Lett.*, 2011, **11**, 2743–2752.
156. T.-G. Cha, B. a Baker, M. D. Sauffer, J. Salgado, D. Jaroch, J. L. Rickus, D. M. Porterfield, and J. H. Choi, *ACS Nano*, 2011, **5**, 4236–4244.
157. S. Wang and S. Si, *Anal. Methods*, 2013, **5**, 2947–2953 |.
158. L. Zhang, T. Li, B. Li, J. Li, and E. Wang, *Chem. Commun. (Camb).*, 2010, **46**, 1476–1478.
159. R. Liu, Z. Chen, Y. Wang, Y. Cui, H. Zhu, P. Huang, W. Li, Y. Zhao, Y. Tao, and X. Gao, *ACS Nano*, 2011, **5**, 5560–5565.
160. D. a Heller, E. S. Jeng, T.-K. Yeung, B. M. Martinez, A. E. Moll, J. B. Gastala, and M. S. Strano, *Science*, 2006, **311**, 508–511.
161. E. S. Jeng, J. D. Nelson, K. L. J. Prather, and M. S. Strano, *Small*, 2010, **6**, 40–43.
162. R. Yang, J. Jin, Y. Chen, N. Shao, H. Kang, Z. Xiao, Z. Tang, Y. Wu, Z. Zhu, and W. Tan, *J. Am. Chem. Soc.*, 2008, **130**, 8351–8358.
163. X. Zhang, K. Jiao, S. Liu, and Y. Hu, *Anal. Chem.*, 2009, **81**, 6006–6012.
164. E. S. Jeng, A. E. Moll, A. C. Roy, J. B. Gastala, and M. S. Strano, *Nano Lett.*, 2006, **6**, 371–375.
165. H. Li, J. Tian, L. Wang, Y. Zhang, and X. Sun, *J. Mater. Chem.*, 2011, **21**, 824–828.
166. G. Pagona, N. Tagmatarchis, J. Fan, M. Yudasaka, and S. Iijima, *Chem. Mater.*, 2006, **18**, 3918–3920.
167. X. Liu, L. Shi, W. Niu, H. Li, and G. Xu, *Biosens. Bioelectron.*, 2008, **23**, 1887–1890.
168. B. Lu, Z. Zhang, J. Hao, G. Xu, B. Zhang, and J. Tang, *Anal. Methods*, 2012, **4**, 3580-3585.
169. G. Xu, L. Gong, H. Dai, X. Li, S. Zhang, S. Lu, Y. Lin, J. Chen, Y. Tong, and G. Chen, *Anal. Methods*, 2013, **5**, 3328.
170. H. Dai, L. Gong, G. Xu, S. Zhang, S. Lu, Y. Jiang, Y. Lin, L. Guo, and G. Chen, *Electrochim. Acta*, 2013, **111**, 57–63.
171. S. Zhu, W. Gao, L. Zhang, J. Zhao, and G. Xu, *Sensors Actuators B Chem.*, 2014, **198**, 388–394.
172. L. Zhang, J. Lei, J. Zhang, L. Ding, and H. Ju, *Analyst*, 2012, **137**, 3126–3131.
173. H. Dai, C. Yang, X. Ma, Y. Lin, and G. Chen, *Chem. Commun. (Camb).*, 2011, **47**, 11915–11917.
174. W. Tu, J. Lei, L. Ding, and H. Ju, *Chem. Commun. (Camb).*, 2009, 4227–4229.
175. F. Xiao, F. Zhao, J. Li, R. Yan, J. Yu, and B. Zeng, *Anal. Chim. Acta*, 2007, **596**, 79–85.
176. J. Zhang, J. Lei, C. Xu, L. Ding, and H. Ju, *Anal. Chem.*, 2010, **82**, 1117–1122.
177. I. Ojeda, B. Garcinuño, M. Moreno-Guzmán, A. González-Cortés, M. Yudasaka, S. Iijima, F. Langa, P. Yáñez-Sedeño, and J. M. Pingarrón, *Anal. Chem.*, 2014, **86**, 7749–7756.
178. F. Yang, J. Han, Y. Zhuo, Z. Yang, Y. Chai, and R. Yuan, *Biosens. Bioelectron.*, 2014, **55**, 360–365.
179. C. Zhao, J. Wu, H. Ju, and F. Yan, *Anal. Chim. Acta*, 2014, **847**, 37–43.
180. H. Dai, S. Zhang, Z. Hong, X. Li, G. Xu, Y. Lin, and G. Chen, *Anal. Chem.*, 2014, **86**, 6418–6424.
181. S. Zhu, S. Han, L. Zhang, S. Parveen, and G. Xu, *Nanoscale*, 2011, **3**, 4589–4592.
182. S. Zhu, Z. Liu, W. Zhang, S. Han, L. Hu, and G. Xu, *Chem. Commun. (Camb).*, 2011, **47**, 6099–6101.
183. S. Zhu, Z. Liu, L. Hu, Y. Yuan, and G. Xu, *Chem. A Eur. J.*, 2012, **18**, 16556–16561.
184. M. Pumera, A. Ambrosi, A. Bonanni, E. L. K. Chng, and H. L. Poh, *TrAC Trends Anal. Chem.*, 2010, **29**, 954–965.
185. Y. Shao, J. Wang, H. Wu, J. Liu, I. A. Aksay, and Y. Lin, *Electroanalysis*, 2010, **22**, 1027–1036.

186. Y. Liu, X. Dong, and P. Chen, *Chem. Soc. Rev.*, 2012, **41**, 2283–2307.
187. T. Gan and S. Hu, *Microchim. Acta*, 2011, **175**, 1–19.
188. R. Hernández, J. Riu, and J. Bobacka, *J. Phys. Chem. C*, 2012, **116**, 22570–22578.
189. J. Ping, Y. Wang, K. Fan, W. Tang, J. Wu, and Y. Ying, *J. Mater. Chem. B*, 2013, **1**, 4781–4791.
190. X.-J. Xing, Y. Zhou, X.-G. Liu, H.-W. Tang, and D.-W. Pang, *Analyst*, 2013, **138**, 6301–6304.
191. X. Yuan, Y. Chai, R. Yuan, Q. Zhao, and C. Yang, *Anal. Methods*, 2012, **4**, 3332–3337.
192. C. Yu, Y. Guo, H. Liu, N. Yan, Z. Xu, G. Yu, Y. Fang, and Y. Liu, *Chem. Commun. (Camb).*, 2013, **49**, 6492–6494.
193. T. Poursaberi, M. R. Ganjali, and M. Hassanisadi, *Talanta*, 2012, **101**, 128–134.
194. W. Tang, J. Ping, K. Fan, Y. Wang, X. Luo, Y. Ying, J. Wu, and Q. Zhou, *Electrochim. Acta*, 2012, **81**, 186–190.
195. P. Noyrod, O. Chailapakul, W. Wonsawat, and S. Chuanuwatanakul, *J. Electroanal. Chem.*, 2014, **719**, 54–59.
196. L. Qiu, H. Zhou, W. Zhu, L. Qiu, J. Jiang, G. Shen, and R. Yu, *New J. Chem.*, 2013, **37**, 3998–4003.
197. Y. Shi, H. Dai, Y. Sun, J. Hu, P. Ni, and Z. Li, *Analyst*, 2013, **138**, 7152–7156.
198. A. Afkhami, H. Khoshsafar, H. Bagheri, and T. Madrakian, *Anal. Chim. Acta*, 2014, **831**, 50–59.
199. B. Devadas, H.-T. Yeh, S.-M. Chen, and S. Piraman, *Electroanalysis*, 2014, **26**, 1712–1720.
200. R. Jain and a. Sinha, *J. Electrochem. Soc.*, 2014, **161**, H314–H320.
201. R. Jain, R. Sharma, R. K. Yadav, and R. Shrivastava, *J. Electrochem. Soc.*, 2013, **160**, H179–H184.
202. N. L. Teradal, P. S. Narayan, A. K. Satpati, and J. Seetharamappa, *Sensors Actuators B Chem.*, 2014, **196**, 596–603.
203. R. Jain and P. Pandey, *J. Electrochem. Soc.*, 2014, **161**, H469–H473.
204. D. Zang, M. Yan, S. Ge, L. Ge, and J. Yu, *Analyst*, 2013, **138**, 2704–2711.
205. S. N. Prashanth, N. L. Teradal, J. Seetharamappa, A. K. Satpati, and a. V. R. Reddy, *Electrochim. Acta*, 2014, **133**, 49–56.
206. B. Devadas, S. Cheemalapati, S.-M. Chen, *RSC Adv.* 2014, **4**, 45895–45902.
207. M. Arvand and N. Ghodsi, *J. Solid State Electrochem.*, 2012, **17**, 775–784.
208. J.-Y. Sun, K.-J. Huang, S.-Y. Wei, and Z.-W. Wu, *Can. J. Chem.*, 2011, **89**, 697–702.
209. S. N. Prashanth, N. L. Teradal, J. Seetharamappa, and a. K. Satpati, *J. Electrochem. Soc.*, 2014, **161**, B117–B122.
210. X. Xing, X. Liu, Y. He, Y. Lin, C. Zhang, H. Tang, and D. Pang, *Biomacromolecules*, 2013, **14**, 117–123.
211. Z. Yin, Q. He, X. Huang, J. Zhang, S. Wu, P. Chen, G. Lu, Q. Zhang, Q. Yan, and H. Zhang, *Nanoscale*, 2012, **4**, 293–297.
212. S. K. Yadav, B. Agrawal, M. Oyama, and R. N. Goyal, *Electrochim. Acta*, 2014, **125**, 622–629.
213. Y. Huang, X. Dong, Y. Shi, C. M. Li, L.-J. Li, and P. Chen, *Nanoscale*, 2010, **2**, 1485–1488.
214. J. Hu, S. Wisetsuwannaphum, and J. S. Foord, *Faraday Discuss.*, 2014, **172**, 457-72.
215. T. E. M. Nancy and V. A. Kumary, *Electrochim. Acta*, 2014, **133**, 233–240.
216. D. Wu, Y. Li, Y. Zhang, P. Wang, Q. Wei, and B. Du, *Electrochim. Acta*, 2014, **116**, 244–249.
217. H. Hosseini, M. Mahyari, A. Bagheri, and A. Shaabani, *Biosens. Bioelectron.*, 2014, **52**, 136–142.
218. F. Zhang, Y. Li, Y. Gu, Z. Wang, and C. Wang, *Microchim. Acta*, 2011, **173**, 103–109.
219. S. Liu, J. Yan, G. He, D. Zhong, J. Chen, L. Shi, X. Zhou, and H. Jiang, *J. Electroanal. Chem.*, 2012, **672**, 40–44.
220. B. Liu, H. T. Lian, J. F. Yin, and X. Y. Sun, *Electrochim. Acta*, 2012, **75**, 108–114.
221. L. Wu, L. Feng, J. Ren, and X. Qu, *Biosens. Bioelectron.*, 2012, **34**, 57–62.
222. P. J. a Borm, D. Robbins, S. Haubold, T. Kuhlbusch, H. Fissan, K. Donaldson, R. Schins, V. Stone, W. Kreyling, J. Lademann, J. Krutmann, D. Warheit, and E. Oberdorster, *The potential risks of nanomaterials: a review carried out for ECETOC.*, 2006, vol. 3.
223. A. Nel, T. Xia, L. Mädler, and N. Li, *Science*, 2006, **311**, 622–627.
224. A. Maynard, R. Aitken, and T. Butz, *Nature*, 2006, **444**, 267–269.
225. C. Buzea, I. I. P. Blandino, and K. Robbie, *Biointerphases*, 2007, **2**, 1–103.
226. V. L. Colvin, *Nat. Biotechnol.*, 2003, **21**, 1166–1171.
227. A. Seaton, L. Tran, R. Aitken, and K. Donaldson, *J. R. Soc. Interface*, 2010, **7**, S119–S129.
228. R. F. Service, *Science*, 1998, **281**, 941.
229. K. Donaldson, R. Aitken, and L. Tran, *Toxicol. Sci.*, 2006, **92**, 5–22.
230. A. Magrez, S. Kasas, V. Salicio, N. Pasquier, J. W. Seo, S. C. Marco Celio, B. Schwaller, and L. Forró, *Nano Lett.*, 2006, **6**, 1121–1125.
231. K. Kostarelos, *Nat. Biotechnol.*, 2008, **26**, 774–776.
232. H. J. Johnston, G. R. Hutchison, F. M. Christensen, S. Peters, S. Hankin, K. Aschberger, and V. Stone, *Nanotoxicology*, 2010, **4**, 207–246.
233. S. Kang, M. Herzberg, D. Rodrigues, and M. Elimelech, *Langmuir*, 2008, **24**, 6409–6413.
234. H. Ali-boucetta and K. Kostarelos, 2008, **1**, 29–32.
235. B. Panessa-Warren, *J. Phys. Condens. Matter*, 2006, **18**, 2185–2201.
236. C. Lam, J. James, M. R, A. S, and H. RL., *Crit Rev Toxicol*, 2006, **36**, 189–217.
237. E. Heister, C. Lamprecht, V. Neves, C. Tîlmaciu, L. Datas, E. Flahaut, B. Soula, P. Hinterdorfer, H. M. Coley, S. R. P. Silva, and J. McFadden, *ACS Nano*, 2010, **4**, 2615–26.
238. N. Saito, H. Haniu, Y. Usui, K. Aoki, K. Hara, S. Takanashi, M. Shimizu, N. Narita, M. Okamoto, S. Kobayashi, H. Nomura, H. Kato, N. Nishimura, S. Taruta, and M. Endo, *Chem. Rev.*, 2014, **114**, 6040–6079.
239. A. M. Schrand, H. Huang, C. Carlson, J. J. Schlager, E. Omacr Sawa, S. M. Hussain, and L. Dai, *J. Phys. Chem. B*, 2007, **111**, 2–7.
240. L. Ding, J. Stilwell, T. Zhang, and O. Elboudwarej, *Nano Lett.*, 2005, **5**, 2448–2464.

241. J. Luszczyn, M. E. Plonska-Brzezinska, A. Palkar, A. T. Dubis, A. Simionescu, D. T. Simionescu, B. Kalska-Szostko, K. Winkler, and L. Echegoyen, *Chem. A Eur. J.*, 2010, **16**, 4870–4880.
242. A. Seabra and A. Paula, *Chem. Res. Toxicol.*, 2014, **27**, 159–168.
243. C. Bussy, H. Ali-Boucetta, and K. Kostarelos, *Acc. Chem. Res.*, 2013, **46**, 692–701.
244. T. Huiquan, K. Yang, Z. Ma, J. Wan, Y. Zhang, Z. Kang, and Z. Liu, *Small*, 2012, **8**, 281–290.
245. X. Ma, L. Jia, L. Zhang, and L. Zhu, *Chem. A Eur. J.*, 2014, **20**, 4072–4073.